



## A springtime comparison of tropospheric ozone and transport pathways on the east and west coasts of the United States.

O.R. Cooper, A. Stohl, S. Eckbart, D.D. Parrish, S.J. Oltmans, B.J. Johnson, P. Nédélec, F.J. Schmidlin, M.J. Newchurch, Y. Kondo, et al.

### ► To cite this version:

O.R. Cooper, A. Stohl, S. Eckbart, D.D. Parrish, S.J. Oltmans, et al.. A springtime comparison of tropospheric ozone and transport pathways on the east and west coasts of the United States.. Journal of Geophysical Research: Atmospheres, 2005, 110 (D5), pp.D05S90. 10.1029/2004JD005183 . hal-00138879

**HAL Id: hal-00138879**

**<https://hal.science/hal-00138879>**

Submitted on 25 Jun 2022

**HAL** is a multi-disciplinary open access archive for the deposit and dissemination of scientific research documents, whether they are published or not. The documents may come from teaching and research institutions in France or abroad, or from public or private research centers.

L'archive ouverte pluridisciplinaire **HAL**, est destinée au dépôt et à la diffusion de documents scientifiques de niveau recherche, publiés ou non, émanant des établissements d'enseignement et de recherche français ou étrangers, des laboratoires publics ou privés.

Copyright

## A springtime comparison of tropospheric ozone and transport pathways on the east and west coasts of the United States

O. R. Cooper,<sup>1,2</sup> A. Stohl,<sup>1,2</sup> S. Eckhardt,<sup>3</sup> D. D. Parrish,<sup>2</sup> S. J. Oltmans,<sup>4</sup> B. J. Johnson,<sup>4</sup> P. Nédélec,<sup>5</sup> F. J. Schmidlin,<sup>6</sup> M. J. Newchurch,<sup>7</sup> Y. Kondo,<sup>8</sup> and K. Kita<sup>9</sup>

Received 30 June 2004; revised 20 October 2004; accepted 15 December 2004; published 15 March 2005.

[1] We have conducted a study to determine the influence of Asian pollution plumes on free tropospheric ozone above the west coast of the United States during spring. We also explored the additional impact of North American emissions on east coast free tropospheric ozone. Long-term ozone monitoring sites in the United States are few, but we obtained ozonesonde profiles from Trinidad Head on the west coast, Huntsville, Alabama, in the southeast, and Wallops Island, Virginia, on the east coast. Additional east coast ozone profiles were measured by the MOZAIC commercial aircraft at Boston, New York City, and Philadelphia. Kilometer-averaged ozone was compared between Trinidad Head and the three east coast sites (MOZAIC, Wallops Island, and Huntsville). Only in the 0–1 km layer did the MOZAIC site have a statistically significant greater amount of ozone than Trinidad Head. Likewise only the 0–1 and 1–2 km layers had greater ozone at Wallops Island and Huntsville in comparison to Trinidad Head. While Wallops Island did show greater ozone than Trinidad Head at 6–9 km, this excess ozone was attributed to a dry air mass sampling bias. A particle dispersion model was used to determine the surface source regions for each case, and the amount of anthropogenic NO<sub>x</sub> tracer that would have been emitted into each air mass. Transport times were limited to 20 days to focus on the impact of direct transport of pollution plumes from the atmospheric boundary layer. As expected, the amount of NO<sub>x</sub> tracer emitted into the east coast profiles was much greater in the lower and mid troposphere than at the west coast. At various altitudes at both coasts there existed a significant positive correlation between ozone and the NO<sub>x</sub> tracer, but the explained variance was generally less than 30%. On the east coast, Wallops Island had the weakest relationship between ozone and the NO<sub>x</sub> tracer, while Huntsville had the strongest. During spring, differences in photochemistry and transport pathways in the lowest 2 km of the troposphere results in an extra 5–14 ppbv of ozone on the east coast in comparison to Trinidad Head. However, despite differing amounts of NO<sub>x</sub> tracer from Asia and North America in the free troposphere, we found no significant difference in free tropospheric ozone between the east and west coasts of the United States during spring.

**Citation:** Cooper, O. R., et al. (2005), A springtime comparison of tropospheric ozone and transport pathways on the east and west coasts of the United States, *J. Geophys. Res.*, 110, D05S90, doi:10.1029/2004JD005183.

<sup>1</sup>Cooperative Institute for Research in Environmental Sciences (CIRES), University of Colorado, Boulder, Colorado, USA.

<sup>2</sup>Aeronomy Laboratory, NOAA, Boulder, Colorado, USA.

<sup>3</sup>Department of Ecology, Technical University of Munich, Freising-Weihenstephan, Germany.

<sup>4</sup>Climate Monitoring and Diagnostics Laboratory, NOAA, Boulder, Colorado, USA.

<sup>5</sup>Laboratoire d'Aérodynamique, CNRS, OMP, Toulouse, France.

<sup>6</sup>NASA Goddard Space Flight Center, Wallops Flight Facility, Wallops Island, Virginia, USA.

<sup>7</sup>Atmospheric Science Department, University of Alabama, Huntsville, Alabama, USA.

<sup>8</sup>Research Center for Advanced Science and Technology, University of Tokyo, Tokyo, Japan.

<sup>9</sup>Department of Environmental Sciences, Ibaraki University, Ibaraki, Japan.

### 1. Introduction

[2] During spring 2002, a partnership of government laboratories and universities conducted the Intercontinental Transport and Chemical Transformation (ITCT-2K2) experiment. This aircraft-based study was designed to intercept and chemically analyze Asian emission plumes transported across the North Pacific Ocean to the western United States (US) (see Parrish *et al.* [2004] and Jaffe *et al.* [2003a, 2003b, 2003c] for summaries of early and recent studies on trans-Pacific transport). During the study three major Asian emission plumes were detected near the US west coast [Nowak *et al.*, 2004], all containing CO in excess of 200 ppbv but with varying ozone/CO relationships (Figure 1). Two of the plumes, intercepted on 5 and 10 May, were transported rapidly from the Asian atmospheric boundary layer (ABL) to North America at relatively

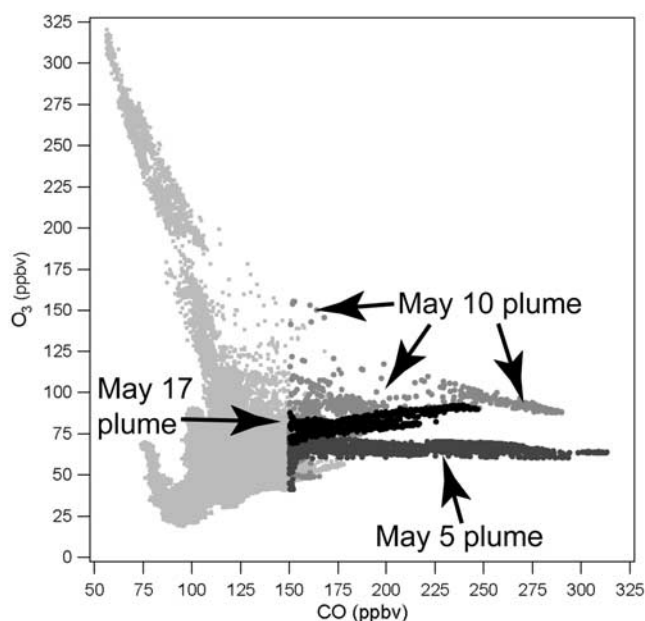


**Figure 1.** All 1-s ozone and CO data from ITCT2K2 flights within free tropospheric, aged air masses above the eastern North Pacific and US west coast. Asian pollution plumes sampled on 5, 10, and 17 May are indicated [after Nowak *et al.*, 2004, Figure 3].

high altitudes and latitudes, with most of the  $\text{NO}_y$  in the form of peroxyacetyl nitrate (PAN), which does not participate in photochemical ozone production during high altitude transport. The 10 May plume was actively mixing with an adjacent stratospheric intrusion, blurring the distinction between trace gases of anthropogenic and stratospheric origin. In contrast, the 17 May plume was measured at lower altitudes and latitudes, with most  $\text{NO}_y$  in the form of  $\text{HNO}_3$ . This was taken to indicate that photochemical processes had converted PAN to  $\text{HNO}_3$  after the air mass left the Asian ABL. The different transport, mixing and photochemical processes that these three plumes had undergone raises the question of what impact Asian pollution plumes have on ozone above the west coast of the US, and their possible impact on east coast ozone as well.

[3] The current understanding of the ozone distribution across the US is as follows. An analysis of ozone measurements at 549 surface sites (mostly urban) across the US showed midafternoon summertime ozone medians are greater in the mid-Atlantic states by at least 10–20 ppbv than at sites in the Pacific Northwest due to the higher emissions of ozone precursors in the east and the relatively cleaner upwind conditions in the west [Fiore *et al.*, 1998]. However, the highest values are found in the Los Angeles Basin of southern California. This same study revealed no significant positive trend in any large region of the country between 1980 and 1995, with large urban areas such as New York, Chicago, and Los Angeles having negative trends due to emission controls. Rural US ozone monitoring sites from 1980 to 1998 have a decreasing trend in high ozone values, but an increasing trend in low  $\text{O}_3$  values, possibly due to an increase in background ozone mixing ratios transported into the country [Lin *et al.*, 2000]. Background ozone levels in

spring measured at five surface sites near the US west coast have increased by about 10 ppbv (30%) over the past 20 years [Jaffe *et al.*, 2003b]. This increase correlates with growing nitrogen oxide emissions in Asia. Although a definite cause and effect relationship has not been established, spring is the season of strongest transport of Asian emissions to the eastern Pacific, so there may be a direct connection.

[4] In terms of free tropospheric ozone, analysis of four ozonesonde stations across the US, (Trinidad Head, California; Boulder, Colorado; Huntsville, Alabama; Wallops Island, Virginia) shows greater ozone mixing ratios at the two eastern sites during all seasons below 500 hPa, with Wallops Island having the greatest values in spring [Newchurch *et al.*, 2003]. Comparison of ozonesonde profiles at Boulder and Wallops Island to the Canadian sites of Edmonton and Goosebay show a decrease of ozone from the US to Canada in the lower half of the troposphere during spring and summer. The Canadian sites show a springtime peak in ozone in the lower half of the troposphere, while the US sites show a broad spring-summer maximum [Logan, 1999].

[5] Several modeling studies have estimated the contribution made by non-US ozone precursors to the US ozone budget [Bernsten *et al.*, 1999; Jacob *et al.*, 1999; Fiore *et al.*, 2002]. Fiore *et al.* [2002] estimated that during summer 1995 chemical production outside of the North American boundary layer contributed an average 25–35 ppbv ozone to afternoon mixing ratios in surface air over the western US, and 15–30 ppbv to the eastern US. Rising Asian anthropogenic emissions between 1985 and 2010 could increase mean ozone concentrations in the western US by 2–6 ppbv [Jacob *et al.*, 1999]. Another study estimates that major Asian pollution events are very common in the mid and upper troposphere above the US, but perhaps only 3–5 of these events directly impact the atmospheric boundary layer along the US west coast during a typical February–May period [Yienger *et al.*, 2000]. Roughly 75% of Asian long-range transport events that impact the NW United States are the result of warm conveyor belt transport in the mid and upper troposphere [Liang *et al.*, 2004]. While Asian dust has been clearly observed at the surface of the US [Jaffe *et al.*, 2003c], no surface observation of ozone or ozone-precursors within the US has so far been distinctly linked to a primary source in Asia.

[6] Exploration of the ozone contrast between the east and west coasts and the transport processes that influence the ozone variation requires as many unbiased ozone profiles as possible over several years. Free tropospheric ozone monitoring on the west coast is only conducted at Trinidad Head, California, where ozonesonde measurements were begun in 1998. Free tropospheric ozone monitoring sites are more numerous on the east coast, but not as extensively as in Europe. These east coast measurements include NASA ozonesondes at Wallops Island, Virginia and NOAA CMDL ozonesondes at Huntsville, Alabama, plus ozone profiles at Boston, New York City (NYC), and Philadelphia measured by commercial aircraft under the European MOZAIC program.

[7] In this study we compare the ozone profiles and transport patterns at Trinidad Head to the east coast sites for the years 2000–2003, focusing on the months of April and May when transport from Asian emission regions is at a maximum [Forster *et al.*, 2004]. The goal is to identify the

**Table 1.** Summary of Ozone Profile Locations and Data Availability

Profile Location	Affiliation	Latitude, Longitude	Time Period April–May Only	Number of Profiles
Trinidad Head	NOAA/CMDL	41.1°N, 124.2°W	2000–2003	54
Boston	MOZAIC	42.5°N, 71.0°W	2000–2002	25
New York City	MOZAIC	40.7°N, 73.6°W	2000–2002	90
Philadelphia	MOZAIC	39.9°N, 72.2°W	2000–2002	19
Wallops Island	NASA/WFF	37.9°N, 75.5°W	2000–2003	38
Huntsville	UAH/ESSC and NOAA/CMDL	34.7°N, 86.6°W	2000–2003	36

surface emission regions with the greatest association to springtime ozone measurements between the surface and 12 km at the US east and west coasts. This analysis is limited to transport times of less than 20 days to study the impact of plumes transported directly from the surface emissions regions to the US troposphere. In section 2 we describe the measurements and modeling techniques applied in this study. In section 3 we compare mean ozone profiles at the east and west coasts and describe the air mass source regions associated with the ozone measurements. Section 4 discusses the influence of transport on east and west coast ozone, and the paper concludes in section 5.

## 2. Method

### 2.1. Ozone Sonde Measurements

[8] Table 1 lists the three ozonesonde stations used in this study and the location of the sites is shown in Figure 2. The National Oceanic and Atmospheric Administration's (NOAA) Climate Monitoring and Diagnostics Laboratory (CMDL) has launched ozonesondes from Trinidad Head, a coastal site in northern California on a weekly basis since 1998 (41.1°N, 124.2°W, 107 m above sea level (a.s.l.)). During special intensive periods to support field campaigns, ozonesondes are launched several times per week or on a daily basis; for example, 29 sondes were launched between 17 April and 20 May 2002, during ITCT-2K2. The balloon-borne ozonesondes were equipped with the widely used and tested electrochemical concentration cell (ECC) sensor [Komhyr, 1969; Komhyr *et al.*, 1995]. ECC sensors have an accuracy of about 10% in the troposphere, except when ozone is less than 10 ppbv when accuracies can be degraded to 15%. Personnel training and instruments were provided by the Ozone and Water Vapor Group of NOAA CMDL. See Oltmans *et al.* [1996], for an explanation of the equipment and techniques employed during this and many other studies. The ozonesondes were prepared with a 2% unbuffered KI solution and produced vertical profiles of ozone, temperature, and frost point between the surface and approximately 35 km a.s.l. The data were partitioned into 100 m vertical layers, and reported as layer averages. Similarly, NOAA CMDL ozonesondes are launched on a weekly basis by the University of Alabama-Huntsville from the Huntsville site (34.7°N, 86.6°W, 196 m a.s.l.) [Newchurch *et al.*, 2003].

[9] Ozonesondes are also launched on a weekly basis from the NASA Wallops Flight Facility (WFF) on Wallops Island, Virginia (37.9°N, 75.5°W, 13 m a.s.l.), as part of the ongoing Upper Air Instrumentation Research Project. These profiles were measured with ECC instruments using

a 1% buffered KI solution, and data are reported at 10-s intervals, or roughly every 50 m. Johnson *et al.* [2002] found that side reactions caused by the buffer in the solution can lead to an overestimation of ozone. NOAA CMDL maintains a Dobson spectrophotometer at WFF that provides column ozone measurements above the site. Comparison of the spectrophotometer column ozone values to those measured by the Wallops Island ozonesondes indicates that, on average, column ozone reported by the ozonesondes is too high by 6%. In this study the Wallops Island ozonesondes have been scaled by the column ozone correction factor calculated by NOAA CMDL from the Dobson spectrophotometer measurements. Without this correction we found that the Wallops Island mean ozone profile was anomalously high through most of the troposphere in comparison to the rest of the sites used in this study. This excess ozone could not be explained by a greater influence from NO<sub>x</sub> emission regions or from the stratosphere.

[10] The practice of correcting the Wallops Island ozonesondes to an independent column ozone measurement has not always been implemented in the past. Oltmans *et al.* [1996] and Logan [1999] did apply the correction to Wallops Island data to account for changes in measurement practices over many years. Thouret *et al.* [1998] did not apply the correction and as discussed in section 2.2, found that below 300 hPa the Wallops Island ozone values were consistently higher than NYC for all months. Newchurch *et al.* [2003] did not use the correction factor, and found that

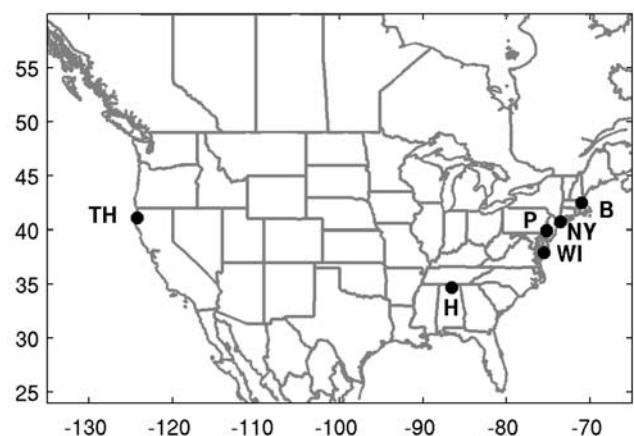


**Figure 2.** Locations of ozone profiles at Trinidad Head (TH), Boston (B), New York City (NY), Philadelphia (P), Wallops Island (WI), and Huntsville (H).

Wallops Island column ozone was on average 1% less than the remotely sensed TOMS column ozone. However, they also found a trend in the relationship with ozonesondes prior to 2000 generally underestimating column ozone, and ozonesondes after 2000 generally overestimating column ozone.

## 2.2. MOZAIC Ozone Profiles

[11] The Measurement of Ozone and Water Vapor by Airbus In-Service Aircraft (MOZAIC) program was initiated by European scientists in 1993 to monitor ozone and water vapor throughout the globe using commercial airliners as measurement platforms [Marenco *et al.*, 1998]. Recently, MOZAIC aircraft have begun to measure CO and NO<sub>y</sub>, but these data were not available in great enough numbers for this study period. Ozone is measured on each aircraft by a dual-beam UV absorption instrument (Thermo-Electron, model 49–103). The response time is 4 s, and the estimated accuracy is  $\pm(2 \text{ ppbv} + 2\%)$  [Thouret *et al.*, 1998]. The data were reported at 150 m intervals. Although the aircraft make measurements for the duration of each flight, we use only the ascent or descent profiles at Boston, New York City, and Philadelphia (Table 1 and Figure 2). The measurements typically extend up to 9 km a.s.l., but the frequency of measurements above this altitude decreases with height as commercial aircraft do not always attain cruising altitudes as high as 10 or 11 km a.s.l. The MOZAIC ascent and descent profiles are considered unbiased with respect to weather or pollutant transport conditions as these commercial aircraft take off and land in all but the most extreme weather conditions.

[12] Thouret *et al.* [1998] compared MOZAIC profiles at NYC (1994–1996) to Wallops Island profiles (1980–1993), separated by a distance of 350 km. Below 300 hPa the Wallops Island ozone values were consistently higher for all months. Comparison of MOZAIC profiles to other nearby ozonesonde stations showed that ozonesondes report about 3–13% more ozone in the free troposphere. Thouret *et al.* noted that this difference is within the range of uncertainty of the two measurement techniques. Parrish *et al.* [2004] compared Trinidad Head ozonesondes to NOAA WP-3D aircraft profiles conducted at approximately the same time and location during ITCT-2K2. From the surface to the midtroposphere, the ozonesonde measurements had relative errors no greater than 2–3 % in comparison to the aircraft profiles and surface ozone measurements at Trinidad Head. These small relative errors show that ozonesonde and aircraft measurements are highly comparable.

## 2.3. Retroplume Calculation

[13] This study relies upon the information provided by retroplumes released from the ozone profiles on the east and west coasts. A retroplume is produced by a Lagrangian or Eulerian transport model and consists of thousands of back trajectory particles released from a particular receptor location. The pathways of all the particles represent the various source regions for a particular air mass at the receptor location. Retroplumes are useful for tracing the origin of an air mass and estimating the amount of time the air mass spent in close proximity to the Earth's surface. Knowledge of this near-surface residence time in conjunction with a global anthropogenic NO<sub>x</sub> emission inventory allows one to esti-

mate the amount of anthropogenic NO<sub>x</sub> emitted into the air mass over a given transport time. Because NO<sub>x</sub> is a precursor of photochemically produced ozone, correlation of the ozone measurements with the NO<sub>x</sub> tracer can provide a qualitative indication of the anthropogenic influence on ozone at a given location. The relatively new retroplume technique was successfully used by Stohl *et al.* [2003a, 2003b] to show that a pollution plume detected above Europe by an instrumented aircraft could be traced to the eastern seaboard of the United States and that the majority of the CO emitted into the air mass originated from the New York City region.

[14] The retroplumes were calculated by the FLEXPART Lagrangian particle dispersion model [Stohl *et al.*, 1998; Stohl and Thomson, 1999], which simulates the transport and dispersion of linear tracers by calculating the trajectories of a multitude of particles. The model has been applied for case studies of trace gas transport [Stohl and Trickl, 1999; Forster *et al.*, 2001; Stohl *et al.*, 2003a; Forster *et al.*, 2004] and a climatology of intercontinental transport [Stohl *et al.*, 2002a; Eckhardt *et al.*, 2003]. The model was driven by the model-level data from the European Centre for Medium-Range Weather Forecasts (ECMWF) [2002], with a temporal resolution of 3 hours (analyses at 0, 6, 12, 18 UTC; 3-hour forecasts at 3, 9, 15, 21 UTC), horizontal resolution of  $1^\circ \times 1^\circ$ , and 60 vertical levels. Particles are transported both by the resolved winds and parameterized subgrid motions. FLEXPART parameterizes turbulence in the boundary layer and in the free troposphere by solving Langevin equations [Stohl and Thomson, 1999]. To account for convection, FLEXPART uses a parameterization scheme [Emanuel and Živković-Rothman, 1999; Seibert *et al.*, 2001].

[15] The retroplume technique is described in detail by Stohl *et al.* [2003a] and Seibert and Frank [2004], and is illustrated in Figure 3. For this example we released 20,000 back trajectory particles from a  $1^\circ \times 1^\circ$  box between 5 and 6 km a.s.l. at Trinidad Head, California. Releases occurred at the launch times of the 32 Trinidad Head ozonesondes during April and May 2002, each release lasting 1 hour. The 32 retroplumes (640,000 total particles) were advected back in time over 20 days. The residence time of the particles in each  $3^\circ \times 5^\circ$  grid cell of the northern hemisphere is determined every 15 min. To account for air density differences between the emission regions and the receptor location, the particle residence times are divided by the air density at each particle's location to yield a specific volume weighted residence time (SVWRT,  $\text{s kg}^{-1} \text{m}^3$ ). Figure 3a shows the average SVWRT distribution for the 32 retroplumes through the entire column of the atmosphere and summed over 20 days of transport. The shading indicates that on average, the highest cumulative SVWRT occurred over the North Pacific and along a band stretching into the midlatitudes of central Asia, as would be expected. To calculate the mass of NO<sub>x</sub> emitted into the retroplume, we focus just on the SVWRT within the so-called footprint layer, which is defined as the 300 m layer of air adjacent to the Earth's surface. Figure 3b shows the average SVWRT distribution for those portions of the 32 retroplumes located within the footprint layer. The surface regions with the strongest transport to the 5–6 km layer above Trinidad Head are the subtropical regions of the North Pacific and the midlatitudes of central Asia. Figure 3c shows the EDGAR 3.2 NO<sub>x</sub> 1995 emission inventory [Olivier and Berndowski,

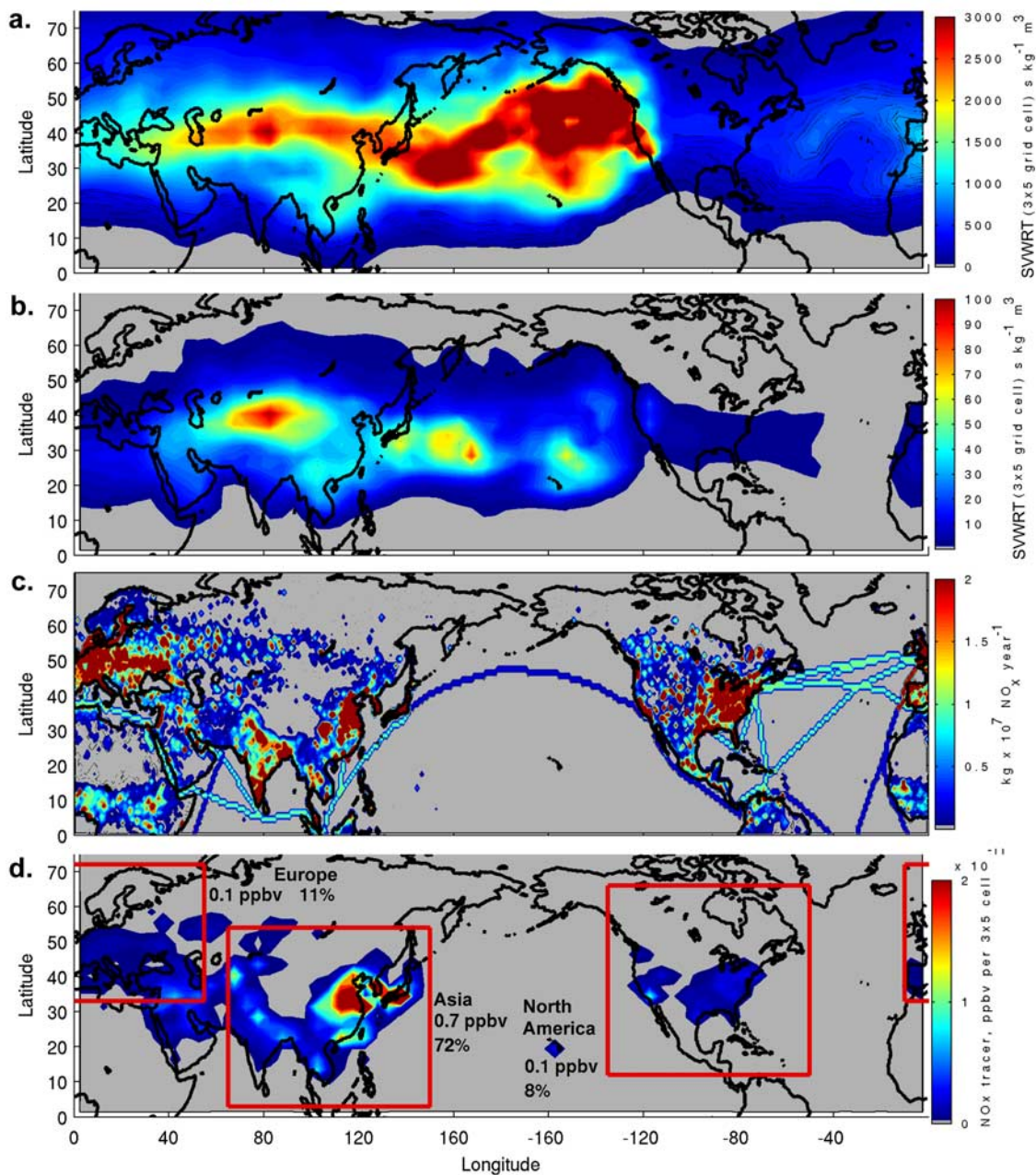


**Figure 3.** Illustration of the retroplume technique. A retroplume was released between 5 and 6 km above Trinidad Head for each of 32 ozonesondes launched during April–May 2002, and allowed to advect for 20 days (each retroplume contained 20,000 particles). (a) The specific volume weighted residence time (SVWRT) of the particles within the atmospheric column was determined and displayed as the average column SVWRT per retroplume. (b) Similarly, the SVWRT of the particles within the 300 m thick footprint layer was determined and displayed as the average footprint layer SVWRT per retroplume. (c) The 1995 EDGAR 1 × 1 degree NO<sub>x</sub> emission inventory. (d) The footprint layer SVWRT values were multiplied by the NO<sub>x</sub> emission inventory to yield the amount of NO<sub>x</sub> tracer (ppbv) emitted into the average retroplume during the previous 20 days. The average retroplume from the 5–6 km layer above Trinidad Head accumulated 1.0 ppbv of NO<sub>x</sub> tracer during the previous 20 days, with 72% from Asia, 11% from Europe, and 8% from North America.

2001]. Multiplying the average SVWRT within the footprint layer (Figure 3b) by the NO<sub>x</sub> emission inventory (Figure 3c) yields the average amount of NO<sub>x</sub> emitted into each retroplume (Figure 3d). In this example the average retroplume is estimated to have accumulated 1.0 ppbv of NO<sub>x</sub> tracer

during the previous 20 days. The red squares in Figure 3d encompass the major emission regions within Europe, Asia, and North America, with 72% of the NO<sub>x</sub> tracer in the 5–6 km layer above Trinidad Head originating from Asia, 11% from Europe, and 8% from North America.

[16] This methodology was applied to all of the ozone profiles, with a retroplume released from a  $1^\circ \times 1^\circ \times 1$  km box at each 1 km interval between the surface and 12 km a.s.l. At the ozonesonde sites of Trinidad Head, Wallops Island, and Huntsville the release boxes were stacked vertically, but for the MOZAIC aircraft profiles the boxes follow the flight tracks as the aircraft ascended or descended. The  $\text{NO}_x$  tracer in this study represents the amount of anthropogenic  $\text{NO}_x$  ( $\text{NO} + \text{NO}_2$ ) emitted into the retroplume during its time in the footprint layer. In a photochemically active environment  $\text{NO}_x$  is rapidly oxidized into various species, such as  $\text{HNO}_3$ ,  $\text{HONO}$ , PAN, and  $\text{N}_2\text{O}_5$ , with the sum of  $\text{NO}_x$  and its oxidation products known as  $\text{NO}_y$ . In the ABL  $\text{NO}_x$  is primarily oxidized to  $\text{HNO}_3$ , which can be removed through wet or dry deposition [Bradshaw *et al.*, 2000]. Because most vertical export out of the ABL is associated with precipitation,  $\text{HNO}_3$  and the other water-soluble  $\text{NO}_y$  species are largely removed via wet deposition during vertical export events. Stohl *et al.* [2002b] report  $\text{NO}_y$  removal efficiencies of 95% and 97% above 3 km during spring and autumn, respectively, downwind of North American emission regions. FLEXPART does not account for the oxidation or removal of  $\text{NO}_x$ . Therefore, the  $\text{NO}_x$  tracer calculated for the ozone profiles above the US is only an estimate of the quantity of  $\text{NO}_x$  emitted into the retroplumes in contact with the emissions regions, and does not provide an estimate of the amount of  $\text{NO}_x$  or  $\text{NO}_y$  actually transported to the locations of the ozone profiles. The  $\text{NO}_x$  tracer is only used to give an indication of the initial pollution level within each retroplume. The retroplumes were limited to 20-days of transport to focus on the direct transport of pollution plumes to the ozone measurement sites. Twenty days is less than the lifetime of ozone or PAN in the mid to upper troposphere, and earlier accumulated  $\text{NO}_x$  may still be present in any particular air mass.

[17] To determine the percentage of a retroplume that originated in the stratosphere, the number of trajectory particles with isentropic potential vorticity (IPV – a quasi conservative dynamic tracer of stratospheric air) greater than 1.5 potential vorticity units (pvu) was tabulated at each 15-min time step. These values were averaged over the 20-day transport period to yield the percentage of the retroplume originating in the lowermost stratosphere, with the tropopause defined as the 1.5 pvu surface.

[18] Position errors associated with individual three-dimensional trajectories, the type used in this study, are typically 20% of the travel distance, and can be much more under critical flow situations [Stohl, 1998]. However, the concept of the retroplume is designed to take into account the uncertainty in source regions as the modeled air mass disperses during backward advection. The uncertainty in the retroplume distribution is, therefore, significantly smaller than the uncertainty of an individual trajectory [Stohl *et al.*, 2002c, 2003a].

### 3. Results

#### 3.1. Comparison of Ozone and $\text{NO}_x$ Tracer Profiles at the East and West Coasts

[19] Figure 4 shows the April–May average ozone profiles for the 6 sites analyzed in this study. The average profiles at the MOZAIC sites of NYC, Boston, and

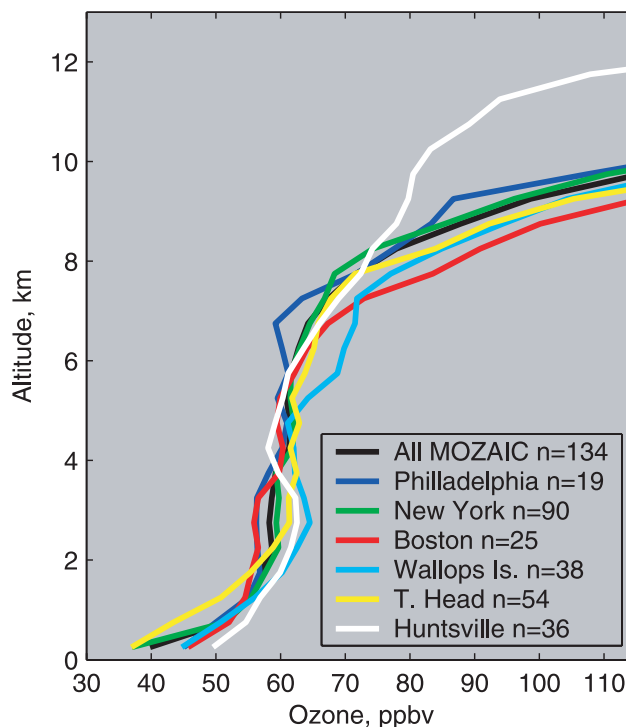


**Figure 4.** Mean ozone profiles for April–May at six locations in the United States. The MOZAIC data (Boston, New York City, and Philadelphia) represent the years 2000–2002, while the other locations represent 2000–2003. Data are reported every 500 m and represent 500 m layer averages.

Philadelphia are fairly similar which is not surprising as all three sites are located in the northeastern US, and are surrounded by high emission regions. Because Philadelphia and Boston have relatively few profiles, we combined them with the NYC profiles into a single site, hereinafter referred to collectively as the MOZAIC sites.

[20] Figures 5, 6, and 7 compare Trinidad Head to each of the three east coast sites: MOZAIC, Wallops Island and Huntsville. Figure 5a shows that km-layer averaged ozone at Trinidad Head is essentially equal to that at the MOZAIC sites, with the exception of the 0–1 km layer where MOZAIC ozone is greater by 5 ppbv. This difference is statistically significant at the 95% confidence interval, according to the Kruskal–Wallace nonparametric one-way analysis of variance test. In terms of transport from the lowermost stratosphere there is no statistically significant difference between the sites (Figure 5b). However, below 9 km there is significantly more  $\text{NO}_x$  tracer associated with the MOZAIC profiles, especially below 4 km.

[21] Comparison of Wallops Island to Trinidad Head shows significantly more ozone at Wallops Island between 0–2 km and between 6–9 km (Figure 6a). Transport from the stratosphere is similar, with the exception of the 0–1 km layer where Trinidad Head has slightly more stratospheric influence (Figure 6b). Below 7 km, Wallops Island has significantly more  $\text{NO}_x$  tracer.

[22] Finally, comparison of Huntsville to Trinidad Head shows significantly more ozone at Huntsville between 0 and 2 km, while Trinidad Head has more ozone above 10 km.

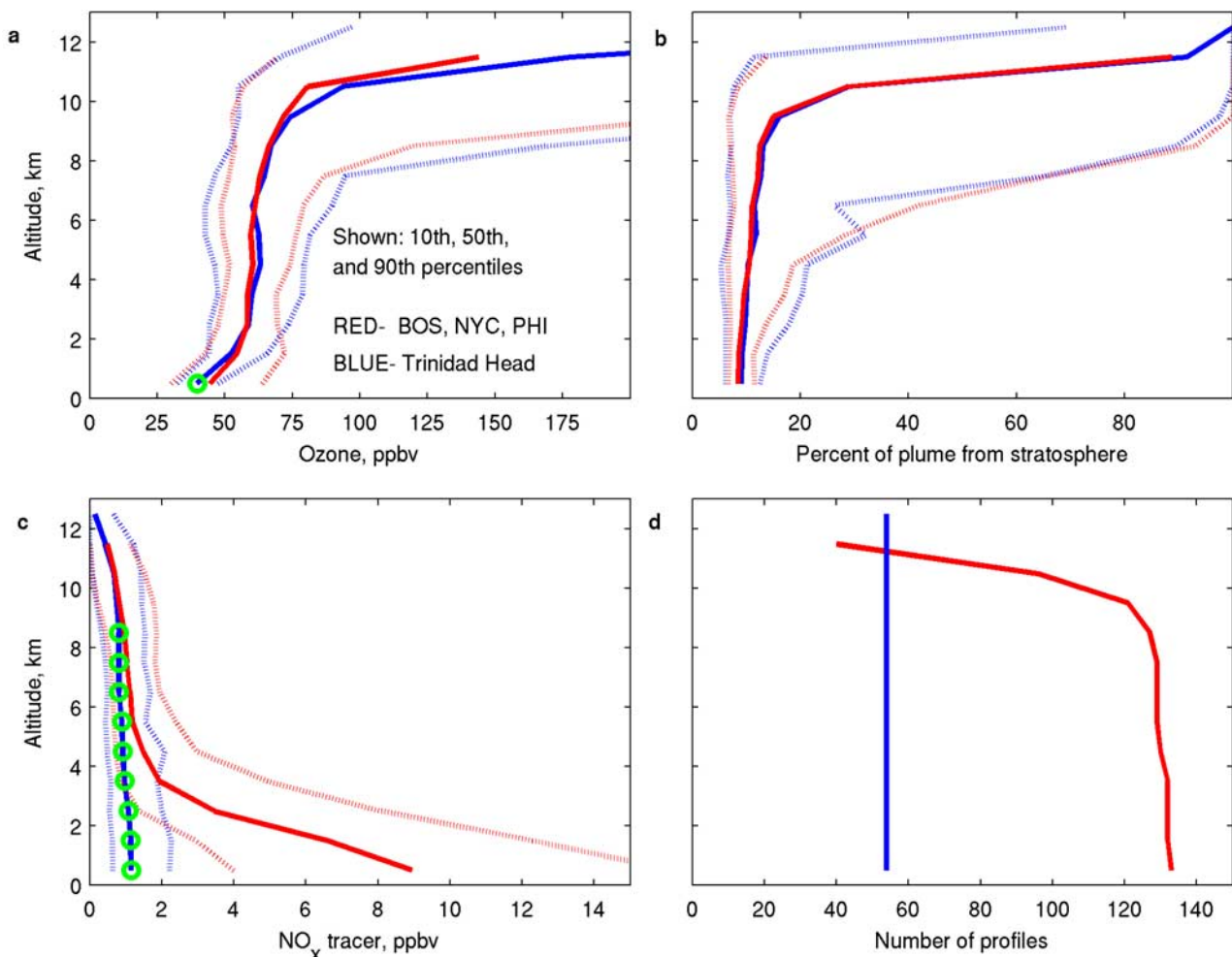


**Figure 5.** (a) Comparison of MOZAIC kilometer average ozone profiles from Boston, New York City, and Philadelphia (red) to Trinidad Head (blue) showing median (solid lines) and 10th and 90th percentiles (dashed lines). Distributions that are significantly different at the 95% confidence interval are indicated by the green circles. (b) Same as in Figure 5a, but for the percent of the retroplume mass that originated in the stratosphere. (c) Same as in Figure 5a, but for the amount of NO<sub>x</sub> tracer accumulated by the retroplumes. (d) The number of ozone profiles available within each kilometer layer.

Above 5 km Trinidad Head has significantly more transport from the stratosphere. The stronger influence of subtropical air masses at Huntsville causes a higher average tropopause and therefore less ozone than Trinidad Head above 10 km. In terms of the NO<sub>x</sub> tracer, Huntsville has greater values below 3 km, while Trinidad Head has slightly greater values between 7 and 9 km.

### 3.2. Comparison of NO<sub>x</sub> Tracer Source Regions for the East and West Coasts

[23] Figure 8 shows the source regions for the NO<sub>x</sub> tracer at four different altitudes above Trinidad Head (Figures 8a–8d), the MOZAIC sites (Figures 8e–8h), and Huntsville (Figures 8i–8l). There are three main similarities between all three sites: (1) The total quantity of NO<sub>x</sub> tracer transported to the receptor sites decreases with altitude. This is primarily the result of the higher altitudes being further removed from the local or regional NO<sub>x</sub> emissions within North America. (2) The percentage of NO<sub>x</sub> tracer from Asia

increases with altitude, while the percentage of NO<sub>x</sub> tracer from North America decreases with altitude. An increase in altitude leads to greater isolation from North American emissions, and transport patterns become more conducive for the direct transport of emissions from Asia to North America. (3) At low altitudes the Asian source regions are dominated by Japan, Korea, and northeast China, but the source regions shift south and west with altitude resulting in increased influence from central China, southeast Asia, and India. Similar results were found by *de Gouw et al.* [2004]. The southwestward shift in source region with altitude is the result of different export mechanisms dominating eastern Asia in comparison to southern and southeast Asia. The emission regions of midlatitude eastern Asia are adjacent to the major region of midlatitude cyclogenesis in the western North Pacific Ocean [Stohl, 2001; Eckhardt et al., 2004]. Springtime emission export from eastern Asia is dominated by midlatitude cyclones with subsequent transport to North America in the lower mid and upper troposphere but with a

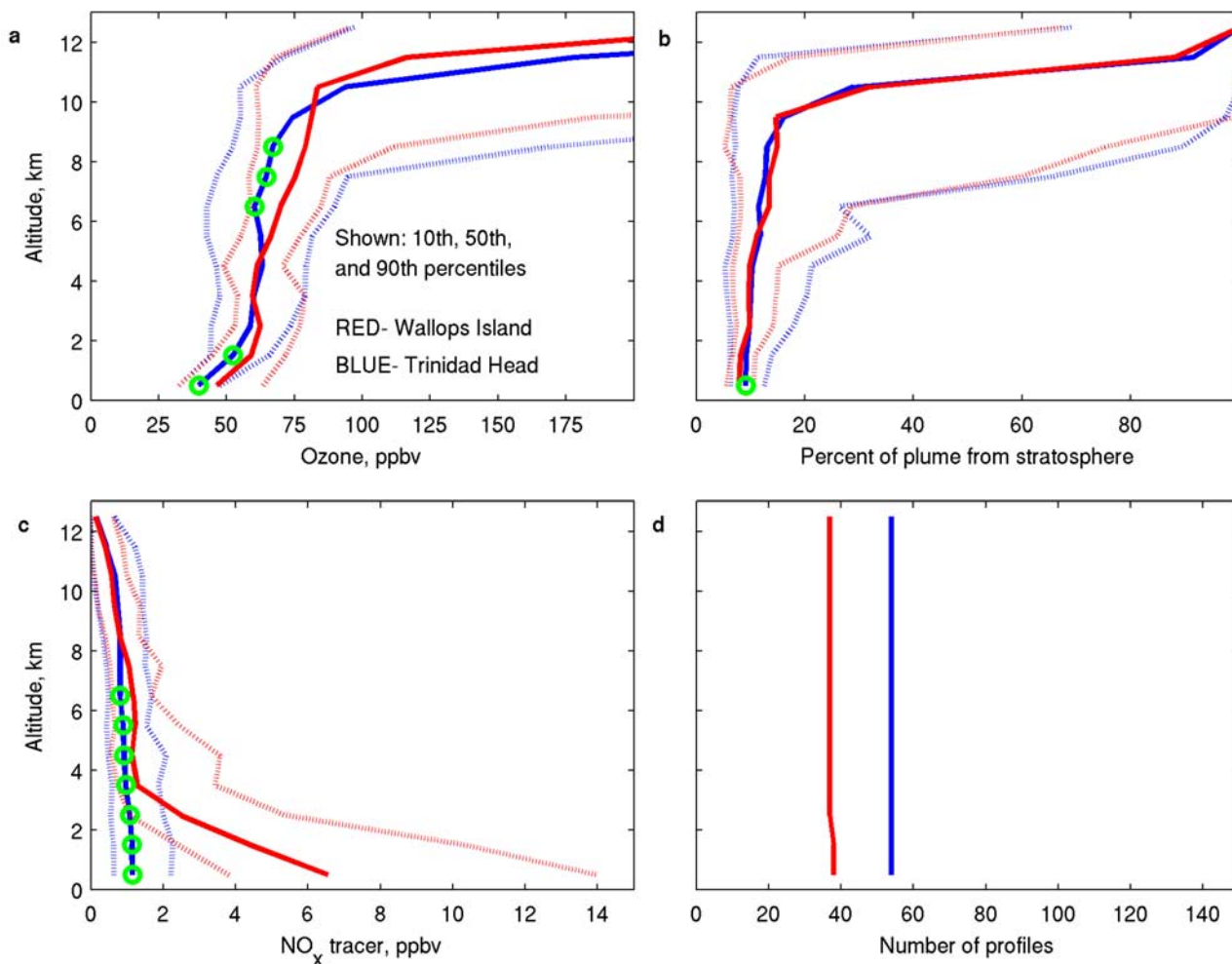


**Figure 6.** As in Figure 5, but for Wallops Island (red) versus Trinidad Head (blue).

maximum in the midtroposphere. In contrast, vertical transport of emissions from India and southeast Asia is dominated by deep convection [Liu *et al.*, 2003; Fuelberg *et al.*, 2003]. The greater equivalent potential temperatures in the southern source regions leads to export at higher altitudes in comparison to the export altitudes of midlatitude cyclones. While cyclones are still important for emission transport in the upper troposphere, the contribution at these altitudes from convective outflow from south and southeast Asia becomes more prominent. Deep convection may be more efficient than WCBs at exporting NO<sub>x</sub> to the free troposphere because the rapid vertical transport is more likely to loft the NO<sub>x</sub> before it is oxidized, in comparison to the much slower vertical motions associated with WCBs.

[24] A similarity between the MOZAIC and Huntsville sites is that the NO<sub>x</sub> tracer source regions within North America also shift toward the south and west with altitude. While deep convection certainly occurs in spring over the eastern US, most of the pollution export is controlled by midlatitude cyclones, which advect east coast emissions to the North Atlantic or northern Canada via diabatic slantwise ascent. Thus, by the time east coast emissions have ascended into the upper troposphere, they are most likely far from the emission regions. Therefore, most of the North America NO<sub>x</sub> tracer in the upper troposphere above the east

coast must originate further upwind. Because the general flow associated with WCBs and springtime deep convection is southwesterly, the associated emission source regions are to the southwest.

[25] Figures 9 and 10 highlight the differences between the sites with regards to NO<sub>x</sub> tracer source region. At most altitudes Trinidad Head has less NO<sub>x</sub> tracer than the east coast sites, with the most notable exceptions being the 10–12 km range at Wallops Island and the 7–10 km range at Huntsville. In the 0–1 km layer the quantity of NO<sub>x</sub> tracer exceeds the Trinidad Head values by a factor of 7, 6, and 4 at MOZAIC, Wallops Island, and Huntsville, respectively. The NO<sub>x</sub> tracer exceeds the Trinidad Head value by at least a factor of 2 from the surface to 6 km at MOZAIC, from the surface to 5 km at Wallops Island, and from the surface to 3 km at Huntsville.

[26] Figure 9 also shows the difference in Asian NO<sub>x</sub> tracer at the 4 sites. Trinidad Head has more Asian NO<sub>x</sub> tracer than the east coast sites at all levels, except for the 6–7 and 7–8 km layers at Wallops Island. At all sites and all levels China is the dominant NO<sub>x</sub> tracer subregion. In general, the Japan/Korea subregion is the second most prominent in the lower half of the troposphere, while India is the second most dominant subregion in the upper half of the troposphere. Southeast Asia only has a small influence

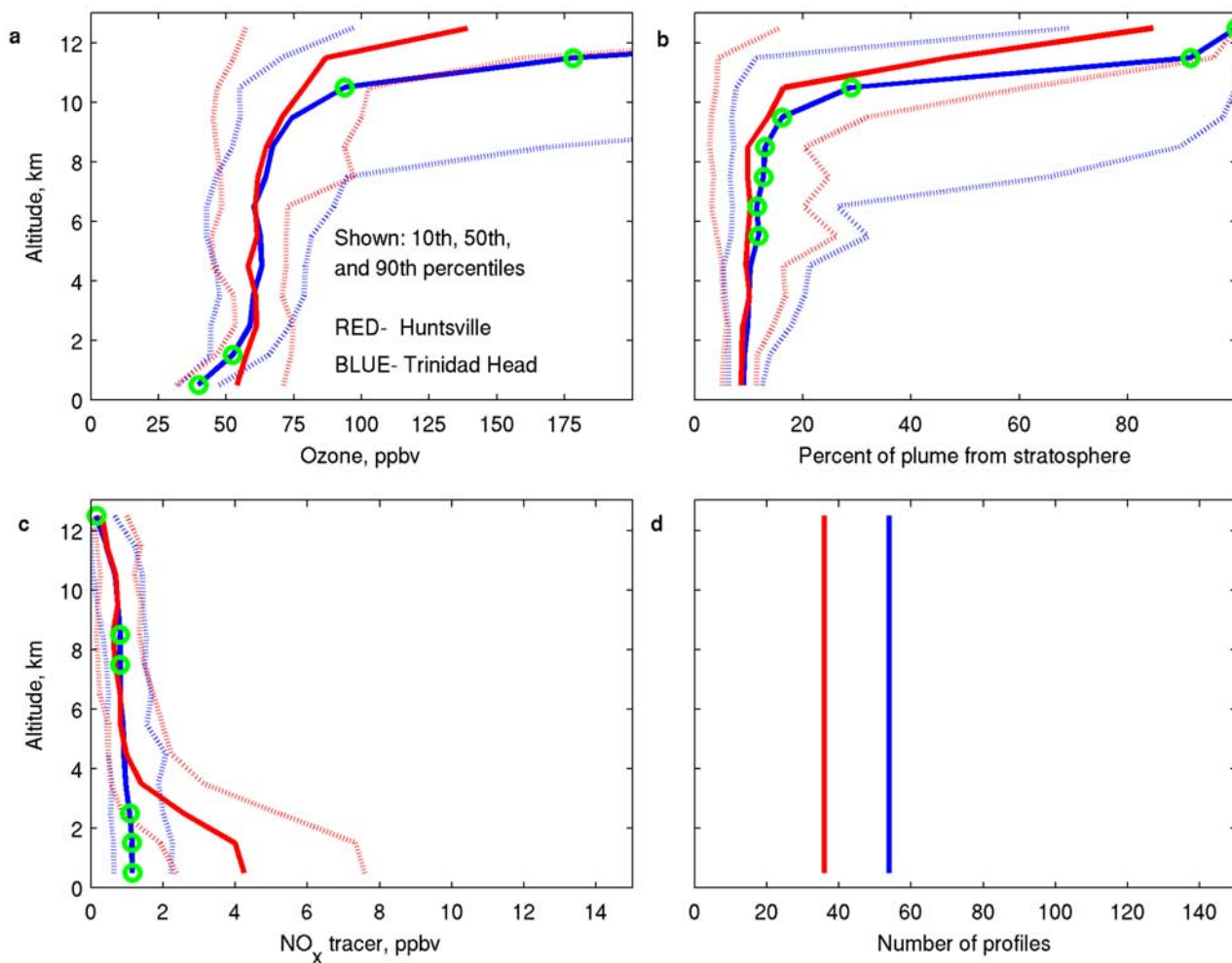


**Figure 7.** As in Figure 5, but for Huntsville (red) versus Trinidad Head (blue).

at any of the 4 sites, reflecting the low emissions from this region (Figure 11a).

[27] Figure 10 shows the difference in North American NO<sub>x</sub> tracer at the three east coast sites. The MOZAIC sites have the most North American tracer at all levels. Neither Wallops Island nor Huntsville is a clear candidate for second place. Interestingly, even though Wallops Island is closer to the higher emissions of the northeast US (Figure 11b), it has less NO<sub>x</sub> tracer than Huntsville between 2 and 8 km. At MOZAIC and Wallops Island, emissions from the northeast US are dominant below 4 km, but above 4 km emissions from the southeast and west make a greater contribution. At Huntsville the southeast makes the single greatest contribution to the total NO<sub>x</sub> tracer below 4 km, but at higher altitudes the west becomes as important as the southeast as a source region.

### 3.3. Relationship Between Ozone and the NO<sub>x</sub> Tracer

[28] Table 2 shows the slope and r-squared value of the relationship between measured ozone and the NO<sub>x</sub> tracer at all four sites, for the altitude layers that have a statistically significant relationship at the 95% confidence interval. Similarly, it shows the relationship between measured ozone and the percentage of the retroplumes that originated in the lowermost stratosphere.

[29] Positive slopes between ozone and the NO<sub>x</sub> tracer are observed at all four sites, at various altitudes implying photochemical production influences the sites at these particular altitudes. In general the slope of the ozone/NO<sub>x</sub> tracer relationship increases with altitude at all four sites. However, this study cannot tell if the greater slope is the result of the high-altitude plumes originating in more photochemically active environments or if the relationship is simply the result of the polluted air being diluted with upper tropospheric or stratospherically influenced air masses containing high levels of background ozone [Cooper *et al.*, 2004]. The r-squared values are not particularly high, with most values well below .50. None of the sites have a significant slope in the 0–1 km layer, possibly due to diurnal variation of near surface ozone as measurements are not always made at midafternoon, and/or due to the fact that model output was only available every 24 hours and, thus, the diurnal variation of NO<sub>x</sub> emissions was not resolved. In addition the MOZAIC near-surface measurements are made in urban areas where NO<sub>x</sub> emissions can lead to ozone titration or production.

[30] Trinidad Head and Huntsville are the sites with the strongest O<sub>3</sub>/NO<sub>x</sub> tracer relationship, each site having 6 layers with significant slopes. Scatterplots of some of the layers at these sites are shown in Figures 12 and 13. The

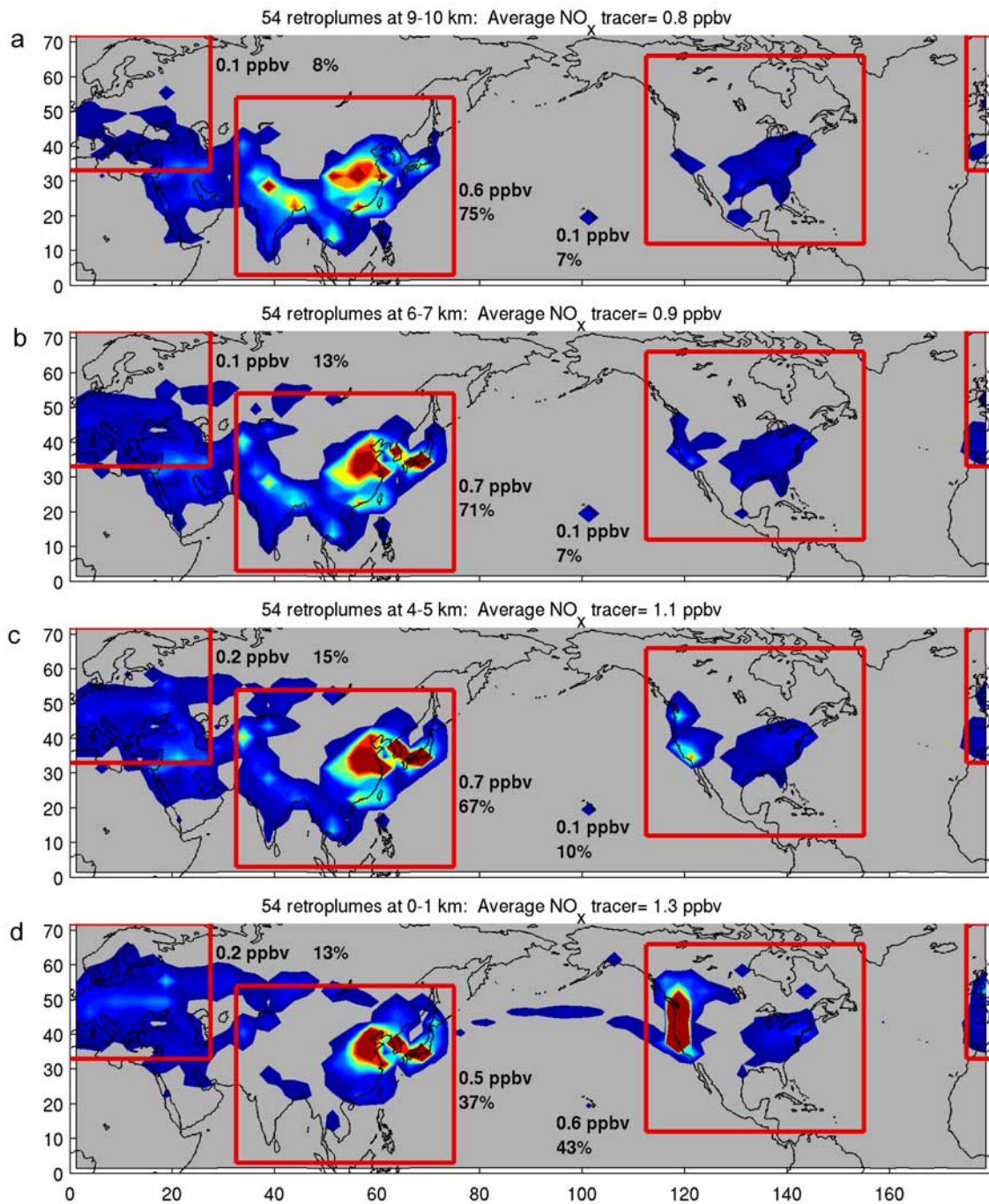


**Figure 8.** The quantity of  $\text{NO}_x$  tracer transported to Trinidad Head at (a) 9–10 km, (b) 6–7 km, (c) 4–5 km, and (d) 0–1 km. The quantity of  $\text{NO}_x$  tracer transported to the MOZAIC sites at (e) 9–10 km, (f) 6–7 km, (g) 4–5 km, and (h) 0–1 km. The quantity of  $\text{NO}_x$  tracer transported to Huntsville at (i) 9–10 km, (j) 6–7 km, (k) 4–5 km, and (l) 0–1 km.  $\text{NO}_x$  tracer source regions are shaded (warmer colors indicating more influential source regions), and the percent and quantity of  $\text{NO}_x$  tracer from Europe, Asia, and North America (regions enclosed within red boxes) are also indicated.

average r-squared value for the significant layers at Trinidad Head is .22, while Huntsville's is .31. The significant layers at Trinidad Head are primarily associated with Asian emissions. At Huntsville only the 8–9 and 9–10 km layers are primarily associated with Asian emissions, with the other four layers primarily associated with North American emissions. Furthermore, Huntsville has more significant

layers in the lower troposphere with relatively high r-squared values, .19–.38. This analysis indicates that any photochemical ozone production at Trinidad Head associated with transport times less than 20 days is mainly influenced by Asia. North America has the major influence at Huntsville below 7 km, with the majority of the emissions from the southeast or western US. The stronger relationship

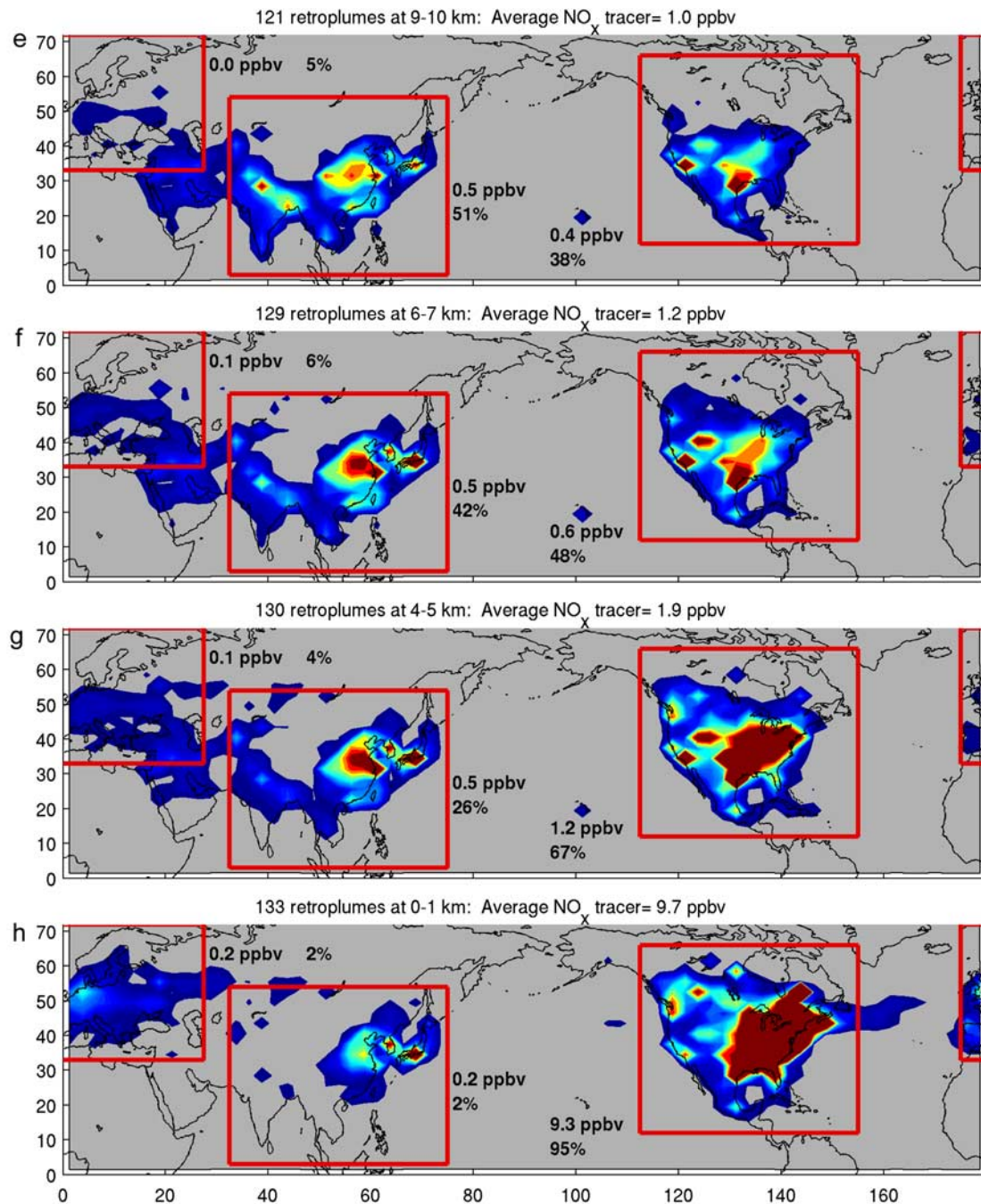


Figure 8. (continued)

at Huntsville is likely the result of (1) shorter distances from the emission source regions to Huntsville resulting in more accurate transport modeling; and (2) Huntsville being closer to the emissions source regions, resulting in less dilution of the polluted air masses with background air masses of various origins.

[31] The MOZAIC sites have 5 layers with significant slopes, but the 4 layers above 2 km only have  $r$ -squared values below .10. The 1–2 km layer has an  $r$ -squared value of 19% and the scatterplot is shown in Figure 14. The significant layers below 4 km at the MOZAIC sites are clearly dominated by North American emissions, with the

majority of the  $\text{NO}_x$  tracer from the northeast US. In contrast, the significant layers in the lower troposphere at Huntsville were dominated by emissions from the southeastern and western US. The more southerly source regions at Huntsville may have allowed a more photochemically active environment, resulting in greater  $r$ -squared values in the lower troposphere of Huntsville.

[32] Only one layer at Wallops Island has a significant slope (Figure 16), located in the upper troposphere where Asian emissions are most prevalent. Despite the large amount of North American  $\text{NO}_x$  tracer below 4 km, none of these layers have a significant slope. While Wallops

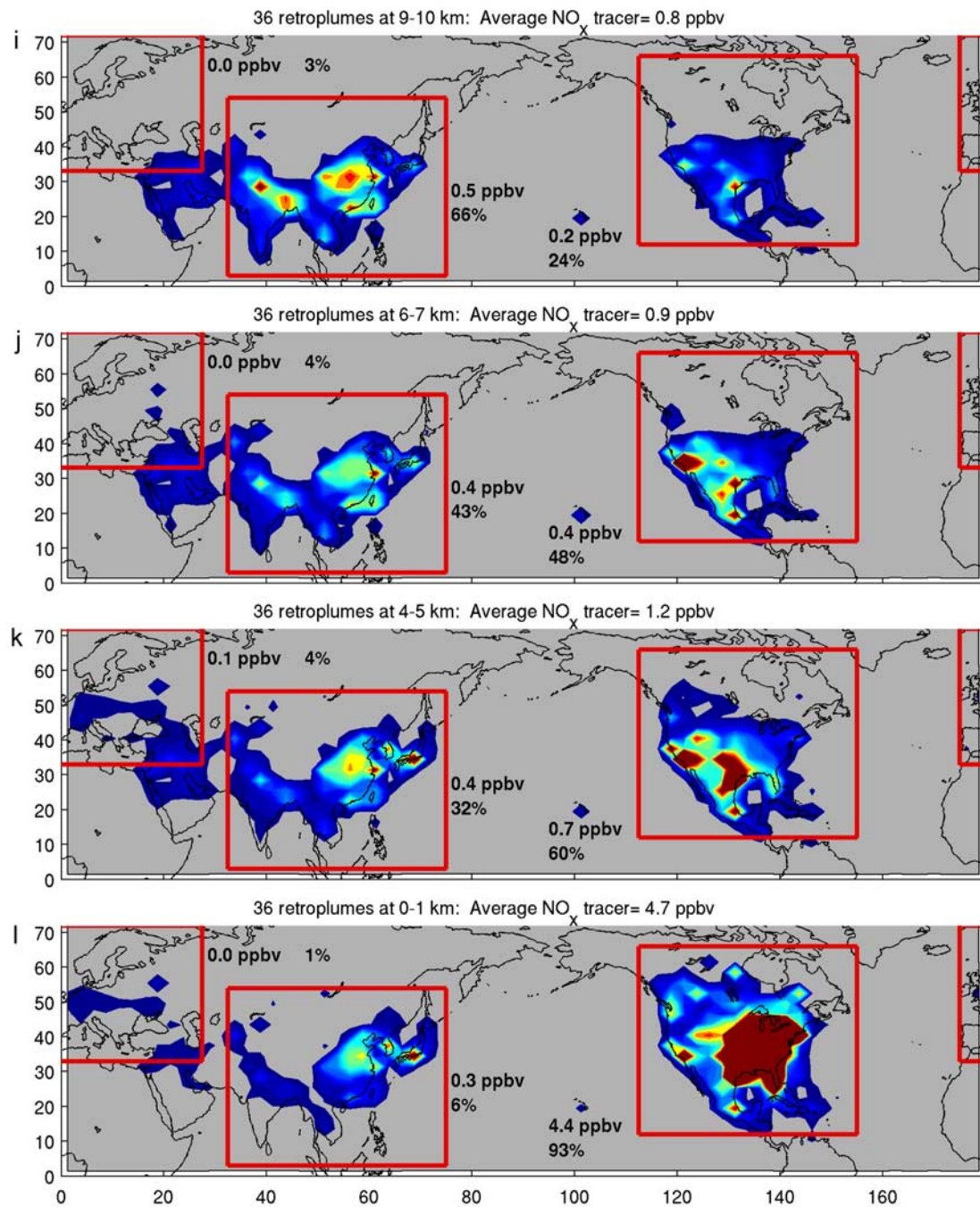


Figure 8. (continued)

Island has significantly more ozone than Trinidad head in the 6–9 km range (Figure 6) the lack of a relationship between ozone and the  $\text{NO}_x$  tracer in the mid and lower troposphere prevents us from concluding that the greater ozone values at Wallops Island are the result of photochemical ozone production associated with transport times less than 20 days.

[33] Table 2 and Figures 12–15 also show the relationship between ozone and the percent of the retroplumes that originated in the lowermost stratosphere. Significant slopes between ozone and the stratospheric tracer are more common than for the ozone/ $\text{NO}_x$  tracer relationship, and in most cases

the r-squared value is greater for the stratospheric tracer, sometimes by a factor of 2 or 3. Cases when the ozone/ $\text{NO}_x$  tracer r-squared value is greater are 11–12 km at Trinidad Head, and 1–4 km at Huntsville. The lowest r-squared values for the stratospheric tracer are in the lower troposphere while maximum values occur around 8–10 km.

[34] There are several reasons for the stronger relationship between ozone and the percent of the retroplumes that originated in the stratosphere, compared to the  $\text{NO}_x$  tracer. In the upper layers the ozone measurements are often made within the stratosphere so this obviously produces a strong stratospheric influence, as illustrated by Figure 16a, which

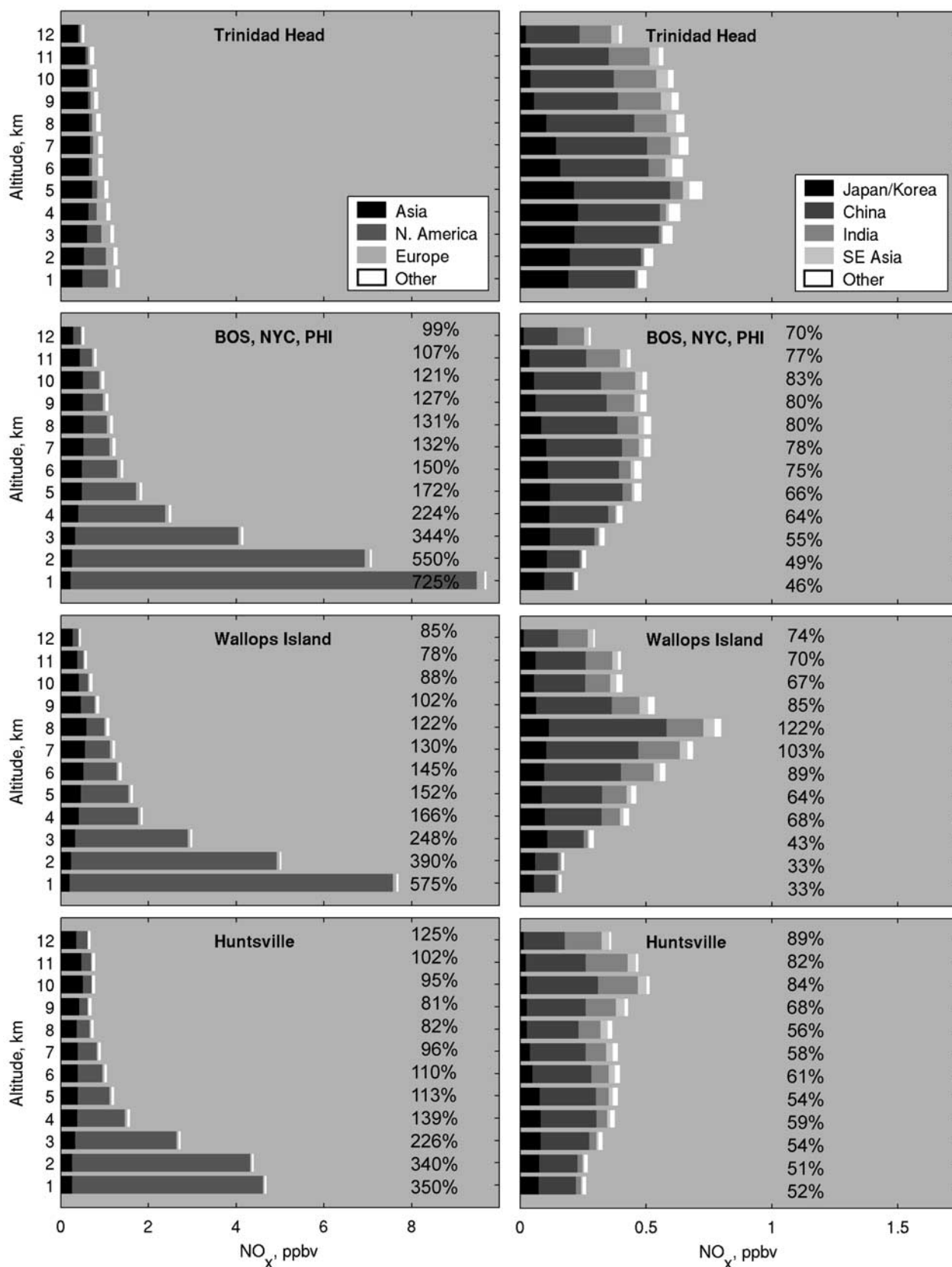


**Figure 9.** (left) Average  $\text{NO}_x$  tracer at the four measurement locations, by altitude, showing the contribution from Asia, North America, and Europe. (right) Average Asia  $\text{NO}_x$  tracer at the four measurement locations, broken down by subregion: Japan/Korea, China, India, and SE Asia. The subregion domains are shown in Figure 11. The percentages compare the amount of  $\text{NO}_x$  tracer at the east coast to the amount at Trinidad Head at each level.

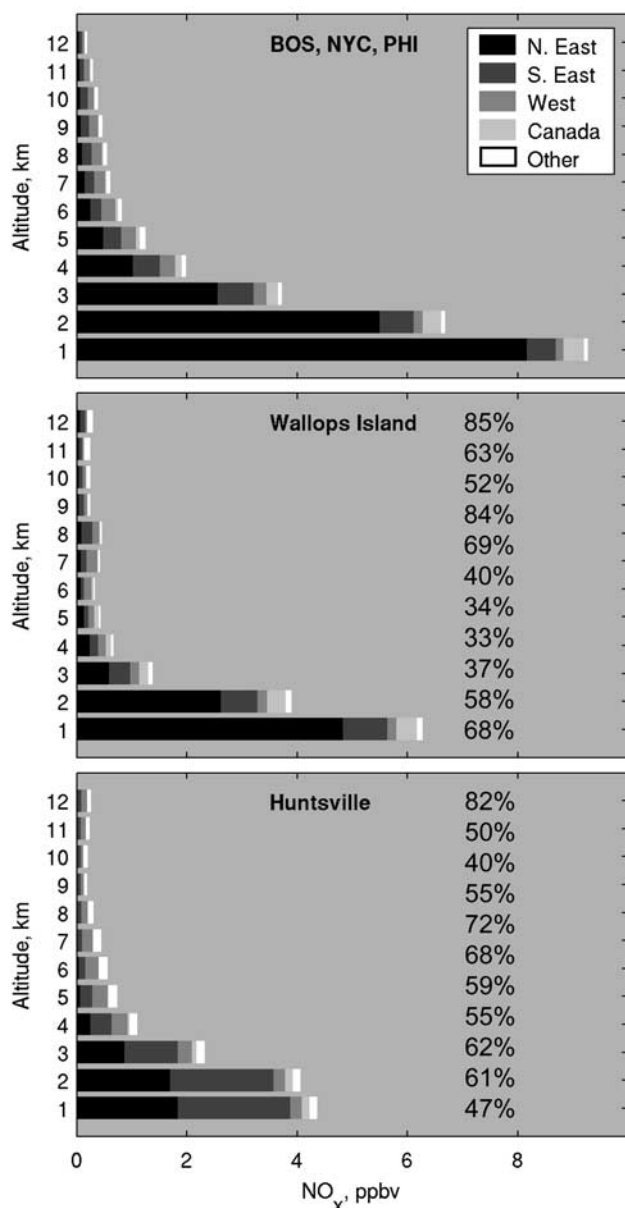


**Figure 10.** Average North America NO<sub>x</sub> tracer at the three east coast measurement locations, broken down by subregion: Northeast, Southeast, West, and Canada. The subregion domains are shown in Figure 11. The percentages compare the amount of NO<sub>x</sub> tracer at Wallops Island or Huntsville to the MOZAIC sites of Boston, New York City, and Philadelphia.

shows the increase of ozone with IPV at Trinidad Head. Below 8 km the measurements are generally made in the troposphere, but portions of the stratosphere are mixed into the troposphere through the breakdown of stratospheric intrusions, which are common events at midlatitudes during spring [Cooper *et al.*, 2002]. The resulting mixture of air often has a major stratospheric component, and due to the very large ozone mixing ratios in the stratosphere, the enhanced ozone can stand out against the background tropospheric ozone more prominently than when polluted boundary layer air is mixed into the free troposphere. Also

the stratosphere is often a closer source region for ozone than many of the emission regions, especially those in Asia (see section 3.4), so the transport of the intrusions is more accurately modeled. Finally, the slope between ozone and the stratospheric tracer can be largely controlled by one event, as shown in Figure 13b.

[35] As with the NO<sub>x</sub> tracer, Trinidad Head and Huntsville have the most layers with significant ozone/stratospheric tracer slopes, and the average *r*-squared values at these sites are greater than at the MOZAIC and Wallops Island sites. The Huntsville *r*-squared values are less than those at Trinidad Head below 4 km. Huntsville is 700 km farther south than Trinidad Head and farther from the polar jet stream where deep stratospheric intrusions form. By the time the intrusions reach the lower troposphere above Huntsville, they have undergone more dilution than those at Trinidad Head (compare Figures 12d and 13c).

### 3.4. Sensitivity Studies

[36] The results presented so far are based on 20 days of transport time and a tropopause defined by the 1.5 pvu surface. We conducted sensitivity studies to determine the influence of shorter transport times and higher tropopause heights.

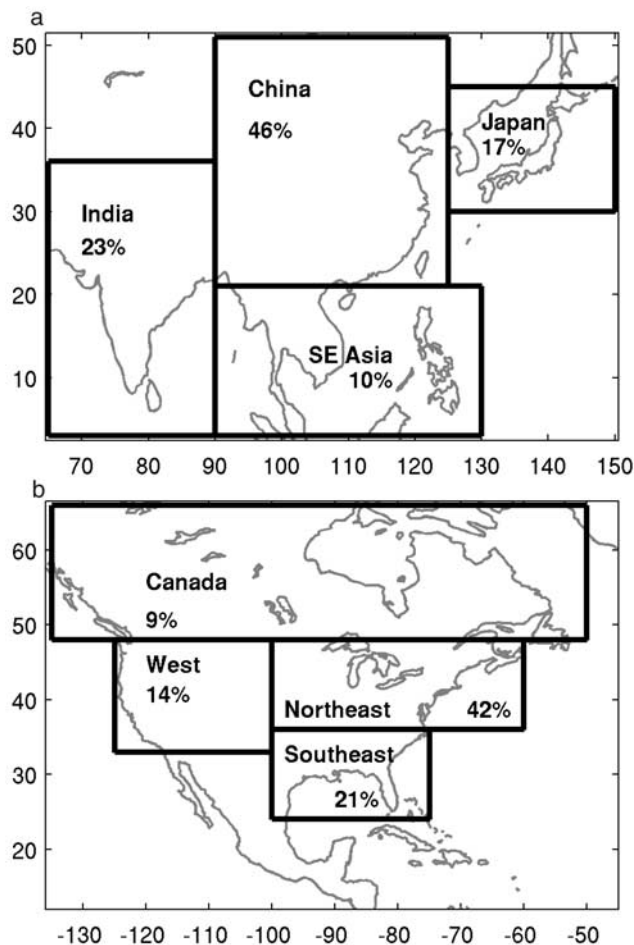


**Figure 11.** Subregions of (a) Asia and (b) North America. Numbers indicate the percent of Asian or North American NO<sub>x</sub> emitted within each subregion.

**Table 2.** Slope and  $r^2$  Value From the Linear Regression of Measured Ozone Against  $\text{NO}_x$  Tracer, and the Linear Regression of Ozone Against the Percent of the Air Mass From the Stratosphere, for Each 1 km Layer at the Four Measurement Locations<sup>a</sup>

Altitude, km	Trinidad Head				MOZAIC			
	O <sub>3</sub> Versus NO <sub>x</sub> Tracer		O <sub>3</sub> Versus Percent From Strat.		O <sub>3</sub> Versus NO <sub>x</sub> Tracer		O <sub>3</sub> Versus Percent From Strat.	
	Slope (ppbv O <sub>3</sub> /ppbv NO <sub>x</sub> )	$r^2$	Slope (ppbv O <sub>3</sub> /‰ strat.)	$r^2$	Slope (ppbv O <sub>3</sub> /ppbv NO <sub>x</sub> )	$r^2$	Slope (ppbv O <sub>3</sub> /‰ strat.)	$r^2$
11–12	32	.52	4.3	.43			3.2	.41
10–11			3.7	.67			2.3	.57
9–10	13	.15	2.5	.73	5	.08	1.6	.60
8–9	12	.17	1.6	.67			1.0	.51
7–8			1.0	.69			0.7	.53
6–7	12	.19	0.9	.57			0.4	.19
5–6	12	.16	0.8	.43	5	.06	0.3	.17
4–5			0.8	.31			0.5	.17
3–4			0.6	.19	1	.08	0.5	.09
2–3	4	.10	0.8	.43	1	.07		
1–2			0.6	.12	2	.19		
0–1								

Altitude, km	Wallops Island				Huntsville			
	O <sub>3</sub> Versus NO <sub>x</sub> Tracer		O <sub>3</sub> Versus Percent From Strat.		O <sub>3</sub> Versus NO <sub>x</sub> Tracer		O <sub>3</sub> Versus Percent From Strat.	
	Slope (ppbv O <sub>3</sub> /ppbv NO <sub>x</sub> )	$r^2$	Slope (ppbv O <sub>3</sub> /‰ strat.)	$r^2$	Slope (ppbv O <sub>3</sub> /ppbv NO <sub>x</sub> )	$r^2$	Slope (ppbv O <sub>3</sub> /‰ strat.)	$r^2$
11–12			3.1	.40			1.1	.45
10–11	16	.26	2.6	.52			1.6	.40
9–10			2.3	.61	27	.50	3.4	.81
8–9			1.5	.64	21	.25	2.9	.85
7–8			0.3	.27			2.1	.75
6–7					9	.26	1.2	.84
5–6							0.6	.55
4–5							0.9	.20
3–4			1.7	.30	4	.19	0.6	.14
2–3					3	.38	1.0	.15
1–2			2.3	.18	3	.27	2.0	.17
0–1								

<sup>a</sup>The regression of ozone against  $\text{NO}_x$  tracer excludes cases with a stratospheric origin greater than 20% by mass. Data are shown only for those relationships that are significant above the 95% confidence interval.

[37] Table 3 shows the slope and  $r^2$  values above Trinidad Head for the relationship between ozone and the  $\text{NO}_x$  tracer and for the relationship between ozone and the percentage of the air mass from the stratosphere. In this case study the tropopause remained at the 1.5 pvu surface, but transport times of 20, 15, 10, and 5 days were analyzed. In general, the number of layers with significant  $\text{O}_3/\text{NO}_x$  tracer slopes and  $r^2$  values decreases as the transport time decreases, due to the fact that Trinidad Head is heavily influenced by Asia and relatively long transport times are required to transport significant amounts of  $\text{NO}_x$  tracer across the Pacific Ocean. The significant layer at 11–12 km disappears when the transport time is shortened from 20 to 15 days.  $\text{NO}_x$  tracer at these altitudes is dominated by transport from south and southeast Asia and apparently 15 days is not long enough for significant amounts of  $\text{NO}_x$  tracer to travel from these regions to Trinidad Head. At 10 days of transport the significant layers are in the midtroposphere which corresponds to the timescale and altitude of trans-Pacific transport by midlatitude cyclones. At 5 days of transport there are no significant layers as this timescale is too short to transport significant amounts of  $\text{NO}_x$  tracer from Asia to Trinidad Head.

[38] In contrast, Table 3 shows that the slope and  $r^2$  values above Trinidad Head for the relationship between ozone and the percent of the air mass from the lower stratosphere changes little with transport time. This finding indicates that

the major stratospheric influence at Trinidad Head occurs within the previous 5 days. The exception is the 1–2 km layer which had a low  $r$ -squared value to begin with but ceases to have a significant relationship at 5 days of transport, indicating that transport times greater than 5 days are required for the stratosphere to influence the lower troposphere above Trinidad Head.

[39] Table 4 is similar to Table 2, but we raised the tropopause threshold from the 1.5 to the 3 pvu surface. In most cases the slope and  $r^2$  values increased for the relationship between ozone and the percent of the air mass from the lower stratosphere. However, for a given altitude, the values changed little with transport time except at the lowest levels. Not surprisingly, a more conservative definition of the tropopause reduced the number of layers with significant relationships between ozone and the  $\text{NO}_x$  tracer and also reduced the corresponding  $r$ -squared values. The  $\text{O}_3/\text{NO}_x$  tracer relationship was only determined for those air masses with less than 20% of their mass originating in the stratosphere. The tropopause is difficult to define and is more like a transition zone than an abrupt boundary, so if we define a higher and more conservative tropopause the likelihood of upper tropospheric air masses containing air with a recent stratospheric origin increases. Therefore this new calculation of the  $\text{O}_3/\text{NO}_x$  tracer relationship has a stronger influence from stratospheric ozone, which overpowers the relationship

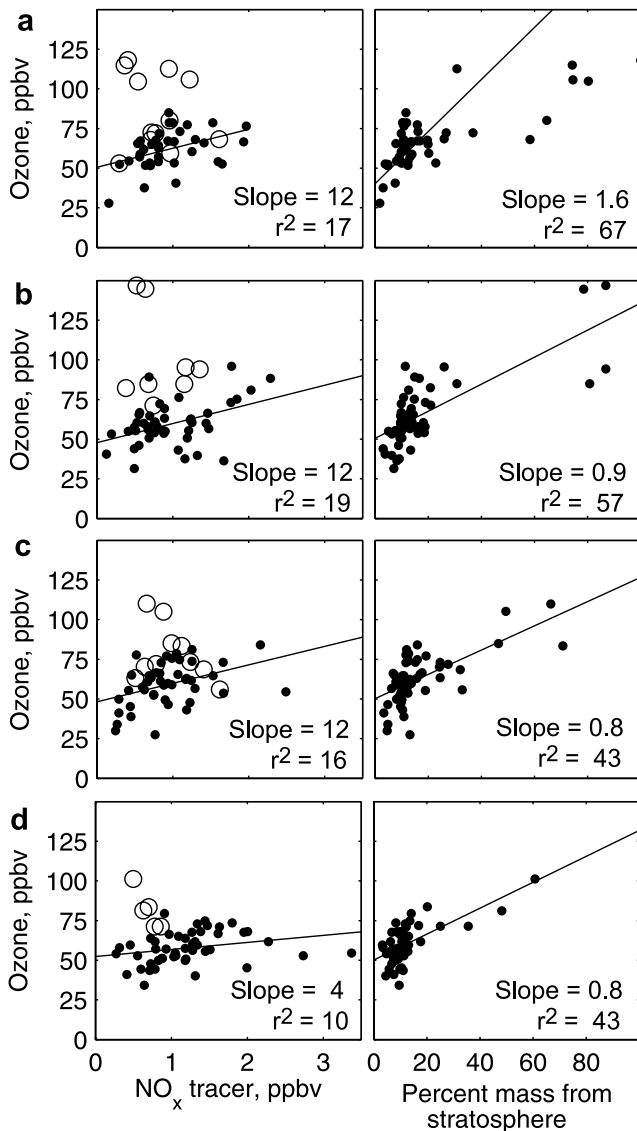


**Figure 12.** Scatterplots of (left) Trinidad Head ozone versus  $\text{NO}_x$  tracer and (right) Trinidad Head ozone versus the percent of the air mass that originated in the lowermost stratosphere at (a) 8–9 km, (b) 6–7 km, (c) 5–6 km, and (d) 2–3 km. Open circles indicate cases in which greater than 20% of the air mass originated in the stratosphere; these cases were excluded from the regression of measured ozone against  $\text{NO}_x$  tracer. Figures 12a (right), 12b (right), and 12d (left) have some points off-scale.

between the  $\text{NO}_x$  tracer and photochemically produced ozone in many layers above Trinidad Head.

[40] Sensitivity tests conducted for the other sites showed similar patterns as described above for Trinidad Head. These tests demonstrate that the 20-day transport time and the 1.5 PV definition of the tropopause are appropriate for this analysis.

#### 4. Discussion

[41] The contrast in lower tropospheric ozone profiles between the west and east coasts of the US is fairly consistent when individually comparing Trinidad Head to

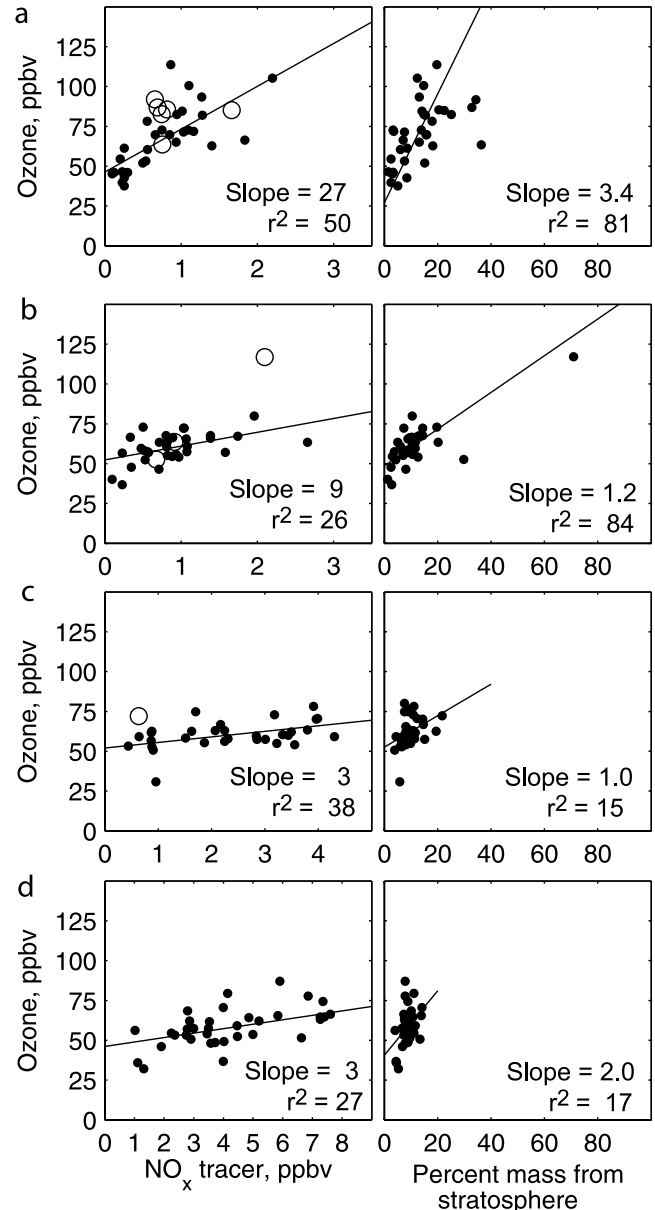


**Figure 13.** As in Figure 12, but for Huntsville at (a) 9–10 km, (b) 6–7 km, (c) 2–3 km, and (d) 1–2 km. Figures 13a (right), 13b (right), 13c (left), and 13d (left) have some points off-scale.

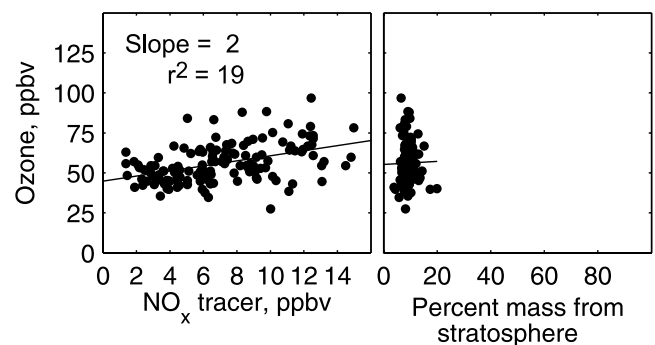


**Figure 14.** As in Figure 12, but for the three MOZAIC sites at 1–2 km.

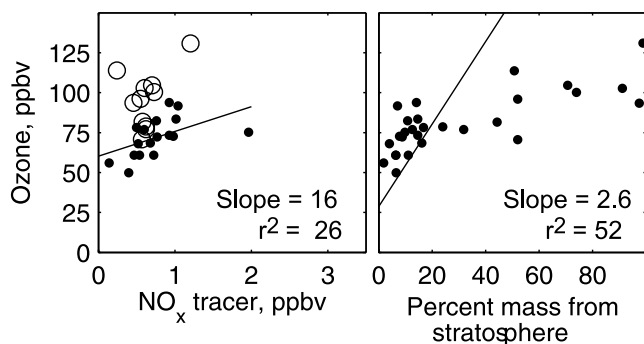


**Figure 15.** As in Figure 12, but for Wallops Island at 10–11 km. The right-hand plot has some points off-scale.

the three east coast sites. Compared to Trinidad Head we found significantly more ozone at the MOZAIC sites between 0–1 km (median ozone is 5 ppbv greater at the MOZAIC sites), while median ozone at Wallops Island was significantly greater than Trinidad Head by 7 ppbv both at 0–1 km, and 1–2 km. Median ozone at Huntsville was significantly greater than Trinidad Head by 14 ppbv at 0–1 km, and 5 ppbv at 1–2 km. We conclude that the extra 5–14 ppbv of ozone in the lowest 2 km of the troposphere in the eastern US is the result of (1) higher  $\text{NO}_x$  emissions in the eastern US contributing to greater photochemical ozone production, and (2) ozone destruction in the North Pacific Ocean marine boundary layer upwind of Trinidad Head.

[42] Along the east coast within the lowest 2 km of the troposphere there is an increase of  $\text{NO}_x$  tracer, but a decrease in ozone, with latitude. We assume that despite the lower  $\text{NO}_x$  tracer values at Wallops Island and Huntsville, the greater ozone values at these sites compared to the MOZAIC sites are due to the southern locations having more sunlight and therefore conditions more conducive for photochemical ozone production.

[43] Above 1 km none of the layers in the MOZAIC profiles contained significantly more ozone than Trinidad Head, despite 8 layers containing significantly more  $\text{NO}_x$  tracer. At Huntsville, between 2 and 10 km no layer contained significantly more ozone than Trinidad Head, despite 3 layers containing significantly more  $\text{NO}_x$  tracer, and despite the 2–3 km layer having one of the stronger ozone/ $\text{NO}_x$ -tracer  $r$ -squared values.

[44] Above 2 km at Wallops Island only the layers between 6–9 km contain significantly more ozone than Trinidad Head even though none of these layers exhibited a significant and positive relationship between ozone and the  $\text{NO}_x$  tracer. Nor did these layers experience significantly more transport from the stratosphere in comparison to Trinidad Head. However, comparison of water vapor mixing ratio (WVMR) at Wallops Island to Huntsville and MOZAIC shows much drier air at Wallops Island between 1 and 10 km, especially in the midtroposphere. We compared WVMR profiles extracted from the NCEP FNL analyses at the times of the Wallops Island ozonesondes to a climatology of NCEP WVMR profiles at 00 and 12 UTC for each day in April and May from 2000 to 2003. The median WVMR profile at the times of the sondes was less than the corresponding climatology profile at all levels. For example, at 3 km (6 km) median WVMR for the

ozonesondes was 85% (75%) of the climatology; and at 3 km (6 km) the 90th percentile WVMR for the ozonesondes was 81% (56%) of the climatology. We compared measured ozone mixing ratios in the lower to mid troposphere associated with WVMR measurements above and below the climatological median and found no large difference. However, between 6–9 km median ozone above Wallops Island is 5–13 ppbv greater when WVMR is less than the climatological median compared to times when WVMR is greater than the median. These ozone differences have a similar magnitude to those between Wallops Island and Trinidad Head. We conclude that the launching of the Wallops Island ozonesondes is biased toward dry conditions and that this dry bias accounts for the greater ozone values at Wallops Island in the 6–9 km range.

[45] While this study has shown that various altitude ranges have a positive relationship between ozone and transport from  $\text{NO}_x$  emissions regions on timescales less than 20 days, the relationship is not particularly strong. Part

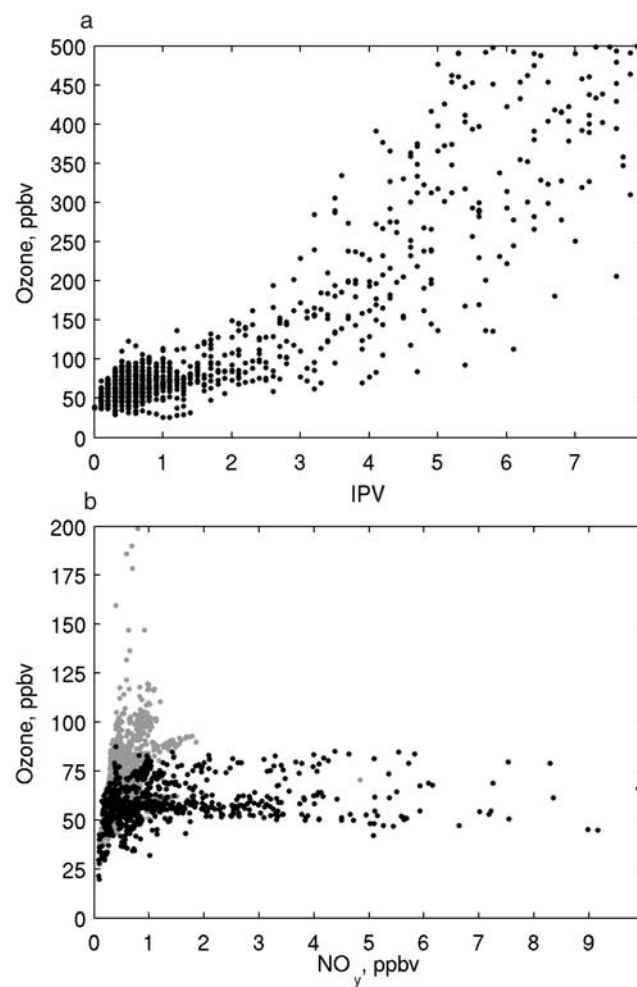


**Figure 16.** (a) Ozone versus IPV at Trinidad Head during April and May 2002 for all altitudes. (b) Ozone versus  $\text{NO}_y$  measured by the PEACE-B program in the vicinity of Japan during April and May 2002. Data measured below 3 km altitude are shaded black, and data measured above 3 km are shaded gray.

**Table 3.** As in Table 2, but for Trinidad Head Only and for Transport Times of 20, 15, 10, and 5 Days

Altitude, km	O <sub>3</sub> Versus NO <sub>x</sub> Tracer								O <sub>3</sub> Versus Percent From Strat.							
	Slope (ppbv O <sub>3</sub> /ppbv NO <sub>x</sub> )				r <sup>2</sup>				Slope (ppbv O <sub>3</sub> /‰ Strat.)				r <sup>2</sup>			
	20 Days	15 Days	10 Days	5 Days	20 Days	15 Days	10 Days	5 Days	20 Days	15 Days	10 Days	5 Days	20 Days	15 Days	10 Days	5 Days
11–12	32				.52				4.3	4.2	4.3	4.1	.43	.42	.42	.42
10–11									3.7	3.7	3.6	3.5	.67	.67	.66	.65
9–10	13	14			.15	.16			2.5	2.4	2.4	2.3	.73	.73	.72	.71
8–9	12	14	17		.17	.19	.17		1.6	1.6	1.5	1.5	.67	.66	.66	.65
7–8									1.0	0.9	0.9	0.9	.69	.69	.68	.65
6–7	12	14	20		.19	.21	.26		0.9	0.8	0.8	0.8	.57	.58	.59	.59
5–6	12	12	17		.16	.15	.14		0.8	0.7	0.7	0.6	.43	.44	.43	.36
4–5		6	7			.08	.09		0.8	0.7	0.7	0.6	.31	.32	.34	.24
3–4									0.6	0.5	0.5	0.4	.19	.19	.19	.16
2–3	4	4			.10	.06			0.8	0.8	0.7	0.6	.43	.44	.44	.36
1–2									0.6	0.5	0.4		.12	.11	.09	
0–1																

of the reason for the weak relationship is due to error within the analysis. While we are confident that FLEXPART reproduces the major motions of the atmosphere and that the retroplume technique accounts for the dispersion of an air parcel advected backward in time, the model and its underlying wind fields cannot reproduce all motions important for intra- and intercontinental transport, with the accurate parameterization of deep convection being especially problematic. Error in this study also arises from the uncertainty of the NO<sub>x</sub> emission inventory. While the EDGAR 3.2 NO<sub>x</sub> 1995 emission inventory [Olivier and Berdowski, 2001] is widely used in atmospheric research, estimates of its uncertainty are roughly 50% or greater (see documentation at <http://arch.rivm.nl/env/int/coredata/edgar/index.html>). Additional uncertainty results from the changes in emissions from 1995 to 2000–2003, the 3° × 5° grid resolution used in the retroplume calculation, and from the diurnal pattern of emissions, which is not accounted for in this study. Furthermore, the emission inventory does not include NO<sub>x</sub> from biomass burning, lightning, or aircraft, and ozone production from these sources could mask the impacts from the NO<sub>x</sub> sources in the inventory, reducing the r-squared terms for the ozone/NO<sub>x</sub> relationship.

[46] Finally, this study does not calculate the photochemical formation of ozone. It simply assumes that greater NO<sub>x</sub> emissions will result in greater ozone production. This is not

always the case as ozone production also varies with the availability of sunlight and hydrocarbons, and in source regions excess NO<sub>x</sub> can result in ozone titration rather than production. Figure 16b shows ozone versus NO<sub>y</sub> measured throughout the ABL and free troposphere above Japan during the PEACE-B study in April–May 2002. Focusing on the lowest 3 km of the atmosphere, it is clear that low ozone corresponds to low NO<sub>y</sub>, but high values of NO<sub>y</sub> (>2 ppbv) are not necessarily associated with high ozone.

[47] What have we learned from this study of ozone measurements that span the major emission regions of North America? As expected, our analysis of the rather limited in situ ozone profile network across the United States found more ozone at the east coast than at the west coast in the lower portions of the troposphere influenced by the atmospheric boundary layer. These results agree with previous studies of surface ozone sites as discussed in the Introduction. However, the ozone measurements indicate that there is no more free tropospheric ozone above the east coast of the United States than above the west coast during spring. This observation is surprising because it does not fit with the model results that suggest the east coast is much more heavily influenced by pollution plumes with transport times less than 20 days. While the correlation between the NO<sub>x</sub> tracer and the measured ozone shows that there is a weak relationship between ozone and direct transport from

**Table 4.** As in Table 3, but for a Tropopause Defined as the 3 PV Surface

Altitude, km	O <sub>3</sub> Versus NO <sub>x</sub> Tracer								O <sub>3</sub> Versus Percent From Strat.							
	Slope (ppbv O <sub>3</sub> /ppbv NO <sub>x</sub> )				r <sup>2</sup>				Slope (ppbv O <sub>3</sub> /‰ Strat.)				r <sup>2</sup>			
	20 Days	15 Days	10 Days	5 Days	20 Days	15 Days	10 Days	5 Days	20 Days	15 Days	10 Days	5 Days	20 Days	15 Days	10 Days	5 Days
11–12									5.0	0.0	4.9		.70	.70	.70	.69
10–11									4.4	4.3	4.2	4.8	.86	.86	.86	.86
9–10									3.0	2.9	2.8	4.1	.86	.86	.85	.85
8–9	11	13	16		.12	.12	.11		2.0	2.0	1.9	2.7	.69	.69	.69	.70
7–8									1.4	1.4	1.3	1.9	.78	.77	.76	.73
6–7	11	12	19		.13	.14	.19		1.2	1.2	1.1	1.2	.60	.60	.60	.57
5–6	10	11	17		.13	.13	.14		1.4	1.3	1.2	1.1	.50	.50	.47	.39
4–5									1.2	1.2	1.1	1.1	.30	.31	.31	.20
3–4									1.0	0.9	0.9	1.0	.20	.20	.20	.18
2–3									1.5	1.4	1.4	1.2	.49	.47	.44	.33
1–2									1.0	0.8	0.6		.16	.12	.08	
0–1																

emission regions, the impact is not enough to significantly increase the east coast ozone above the springtime background ozone. This appears to be the crux of the issue. The lifetime of ozone in the free troposphere is much longer than 20 days during springtime. Furthermore, free tropospheric ozone in the northern hemisphere is strongly influenced by the broad background increase in photochemical ozone production that occurs every spring [Atlas *et al.*, 2003; Emmons *et al.*, 2003] as well as by stratospheric intrusions that occur frequently throughout the midlatitudes. We conclude that rapidly transported pollution plumes with varying degrees of photochemical ozone production and loss, that inevitably mix with free tropospheric air containing relatively long-lived background ozone, play a minor role in influencing the overall tropospheric ozone burden above a particular site. In addition, we cannot attribute the ozone burden above a site to any primary upwind emission region, either on the regional or continental scale. Rather, the ozone burden above a site is the complicated result of varying photochemical and transport processes on timescales shorter and greater than 20 days. The multiyear ozone measurements gathered for this study and our model analysis agrees with recent studies that conclude that distinct long range transport events impacting the western United States do not always correlate well with ozone measurements [Yienger *et al.*, 2000; Jaeglé *et al.*, 2003; Jaffe *et al.*, 2003a; Nowak *et al.*, 2004]. The current study goes further in demonstrating that the same applies to the eastern United States despite the closer proximity to major emission regions.

## 5. Conclusions

[48] The major conclusion from this analysis of springtime ozone measurements at one west coast (Trinidad Head) and three east coast sites (MOZAIC, Wallops Island, and Huntsville) is that there is only a weak relationship between tropospheric ozone and direct transport (<20 days) from  $\text{NO}_x$  emission regions. In general, the quantity of  $\text{NO}_x$  tracer at Trinidad Head, MOZAIC, and Wallops Island explains less than 20% of the ozone variance as estimated from the  $r^2$  values, while the relationship at Huntsville is slightly stronger, perhaps due to the more southerly  $\text{NO}_x$  source regions. North American emissions are associated with the higher east coast ozone mixing ratios in the lowest 1 or 2 km of the troposphere. However, in the free troposphere direct transport from neither North American nor Asian emission regions appears to have a strong relationship to ozone. Transport from the lowermost stratosphere explains more of the ozone variance but mainly in the mid and upper troposphere. More specific results are as follows:

[49] 1. During spring, differences in  $\text{NO}_x$  availability, photochemistry, and transport pathways in the lowest 2 km of the troposphere results in an extra 5–14 ppbv of ozone on the east coast in comparison to Trinidad Head. Above 2 km there is no more ozone above the east coast compared to Trinidad Head even though many layers above the east coast are associated with greater amounts of  $\text{NO}_x$  tracer. The excess ozone at 6–9 km above Wallops Island is believed to be the result of a dry air mass bias in the sampling.

[50] 2. In terms of  $\text{NO}_x$  tracer source regions at all four sites: The total quantity of  $\text{NO}_x$  tracer decreases with altitude, and the percentage of  $\text{NO}_x$  tracer from Asia increases with altitude, while the percentage of  $\text{NO}_x$  tracer from North America decreases with altitude. At low altitudes the Asian source regions are dominated by Japan, Korea, and northeast China, but the source regions shift south and west with altitude, resulting in increased influence from central China, southeast Asia, and India.

[51] 3. A similarity between the east coast sites is that the  $\text{NO}_x$  tracer source regions within North America shift toward the south and west with altitude.

[52] 4. At most altitudes, Trinidad Head has less  $\text{NO}_x$  tracer than the east coast sites. In the 0–1 km layer the quantity of  $\text{NO}_x$  tracer exceeds the Trinidad Head values by a factor of 7, 6, and 4 at MOZAIC, Wallops Island, and Huntsville, respectively.

[53] 5. Positive slopes between ozone and the  $\text{NO}_x$  tracer are observed at all four sites, at various altitudes implying photochemical production influences the sites at these particular altitudes. The  $r$ -squared values are not particularly high, with most values well below .50. None of the sites have a significant slope in the 0–1 km layer.

[54] 6. Trinidad Head and Huntsville are the sites with the strongest  $\text{O}_3/\text{NO}_x$  tracer relationship, each site having 6 layers with significant slopes. Asia is the major  $\text{NO}_x$  tracer source region at Trinidad Head. North America has the major influence at Huntsville below 7 km, with the majority of the emissions from the southeast or western US.

[55] 7. The only layer at the MOZAIC sites with a relatively strong  $\text{O}_3/\text{NO}_x$  slope is the 1–2 km layer, which is dominated by emissions from the northeast US.

[56] 8. Despite the large amount of North American  $\text{NO}_x$  tracer below 4 km at Wallops Island, none of these layers have significant  $\text{O}_3/\text{NO}_x$  slopes.

[57] 9. Significant slopes between ozone and the stratospheric tracer are more common than for the ozone/ $\text{NO}_x$  tracer relationship, and in most cases the  $r$ -squared value is greater for the stratospheric tracer, sometimes by a factor of 2 or 3.

[58] A common conclusion of studies focused on the spatial and temporal variability of free tropospheric trace gases is that available measurements are inadequate to provide a full characterization. We draw the same conclusion for this study of ozone source regions above the US, especially for the west coast where the lone site of Trinidad Head provides no information on the west coast ozone latitudinal variation. The study of ozone variability above the US is confounded by the fact that ozone has a strong springtime source from both anthropogenic and stratospheric source regions. Simultaneous measurements of CO would be invaluable for separating the influence from stratospheric and anthropogenic sources. The MOZAIC program has begun to measure CO and  $\text{NO}_y$  on some of its flights, and over time enough data will become available to allow us to separate the source regions, at least for the northeast US where measurements are most frequent. The current frequency of MOZAIC measurements in the northeast US is adequate for addressing the interannual variability of ozone, but the measurement frequency at the ozonesonde sites is not. Logan [1999] recommended that 20 profiles are required at a

given extratropical location to ensure ozone monthly means are reliable to better than  $\pm 15\%$  for 800–500 hPa at the 95% confidence interval. Given that standard operating procedures provide four ozonesonde profiles per month, a factor of five increase in launch frequency is necessary to meet Logan's recommendation. While the European funded measurement of free tropospheric trace gases fills some of the holes in the US monitoring program, we could learn much more if US programs could monitor ozone and anthropogenic trace gases in the free troposphere several times per week at key locations across the country.

[59] **Acknowledgments.** The ITCT 2K2 campaign was conducted under the framework of the IGAC (International Global Atmospheric Chemistry) project (<http://www.igac.noaa.gov/>). The Edgar NO<sub>x</sub> emission inventory was obtained online from <http://arch.rivm.nl/env/int/coredata/edgar/index.html>. The EDGAR project is a product of the National Institute for Public Health (RIVM) and the Netherlands Organisation for Applied Scientific Research (TNO), and is linked into and part of the Global Emissions Inventory Activity (GEIA) of IGBP/IGAC. We thank John Nowak, Cooperative Institute for Research in Environmental Sciences (CIRES), University of Colorado, for providing Figure 1. Access to the ECMWF data was provided by ECMWF and Deutscher Wetterdienst.

## References

- Atlas, E. L., B. A. Ridley, and C. A. Cantrell (2003), Tropospheric Ozone Production about the Spring Equinox (TOPSE) Experiment: Introduction, *J. Geophys. Res.*, **108**(D4), 8353, doi:10.1029/2002JD003172.
- Berntsen, T. K., S. Karlsdóttir, and D. A. Jaffe (1999), Influence of Asian emissions on the composition of air reaching the northwestern United States, *Geophys. Res. Lett.*, **26**, 2171–2174.
- Bradshaw, J., D. Davis, G. Grodzinsky, S. Smyth, R. Newell, S. Sandholm, and S. Liu (2000), Observed distributions of nitrogen oxides in the remote free troposphere from the NASA Global Tropospheric Experiment programs, *Rev. Geophys.*, **38**, 61–116.
- Cooper, O. R., J. L. Moody, D. D. Parrish, M. Trainer, J. S. Holloway, G. Hübler, F. C. Fehsenfeld, and A. Stohl (2002), Trace gas composition of midlatitude cyclones over the western North Atlantic Ocean: A seasonal comparison of ozone and CO, *J. Geophys. Res.*, **107**(D7), 4057, doi:10.1029/2001JD000902.
- Cooper, O. R., et al. (2004), On the life-cycle of a stratospheric intrusion and its dispersion into polluted warm conveyor belts, *J. Geophys. Res.*, **109**, D23S09, doi:10.1029/2003JD004006.
- de Gouw, J. A., et al. (2004), Chemical composition of air pollution transported from Asia to the U.S. west coast during ITCT-2K2: Fossil fuel versus biomass burning signatures, *J. Geophys. Res.*, **109**, D23S20, doi:10.1029/2003JD004202.
- Eckhardt, S., A. Stohl, S. Beirle, N. Spichtinger, P. James, C. Forster, C. Junker, T. Wagner, U. Platt, and S. Jennings (2003), The North Atlantic Oscillation controls air pollution transport to the Arctic, *Atmos. Chem. Phys.*, **3**, 1769–1778.
- Eckhardt, S., A. Stohl, H. Wernli, P. James, C. Forster, and N. Spichtinger (2004), A 15-year climatology of warm conveyor belts, *J. Clim.*, **17**, 218–237.
- Emanuel, K. A., and M. Živković-Rothman (1999), Development and evaluation of a convection scheme for use in climate models, *J. Atmos. Sci.*, **56**, 1766–1782.
- Emmons, L. K., et al. (2003), Budget of tropospheric ozone during TOPSE from two chemical transport models, *J. Geophys. Res.*, **108**(D8), 8372, doi:10.1029/2002JD002665.
- European Centre for Medium-Range Weather Forecasts (ECMWF) (2002), IFS documentation, edited by P. W. White, Reading, UK.
- Fiore, A. M., D. J. Jacob, J. A. Logan, and J. H. Yin (1998), Long-term trends in ground level ozone over the contiguous United States, 1980–1985, *J. Geophys. Res.*, **103**, 1471–1480.
- Fiore, A. M., D. J. Jacob, I. Bey, R. M. Yantosca, B. D. Field, and A. C. Fusco (2002), Background ozone over the United States in summer: Origin, trend, and contribution to pollution episodes, *J. Geophys. Res.*, **107**(D15), 4275, doi:10.1029/2001JD000982.
- Forster, C., et al. (2001), Transport of boreal forest fire emissions from Canada to Europe, *J. Geophys. Res.*, **106**, 22,887–22,906.
- Forster, C., et al. (2004), Lagrangian transport model forecasts and a transport climatology for the Intercontinental Transport and Chemical Transformation 2002 (ITCT 2K2) measurement campaign, *J. Geophys. Res.*, **109**, D07S92, doi:10.1029/2003JD003589.
- Fuelberg, H. E., C. M. Kiley, J. R. Hannan, D. J. Westberg, M. A. Avery, and R. E. Newell (2003), Meteorological conditions and transport pathways during the Transport and Chemical Evolution over the Pacific (TRACE-P) experiment, *J. Geophys. Res.*, **108**(D20), 8782, doi:10.1029/2002JD003092.
- Jacob, D. J., J. A. Logan, and P. P. Murti (1999), Effect of rising Asian emissions on surface ozone in the United States, *Geophys. Res. Lett.*, **26**, 2175–2178.
- Jaeglé, L., D. A. Jaffe, H. U. Price, P. Weiss-Penzias, P. I. Palmer, M. J. Evans, D. J. Jacob, and I. Bey (2003), Sources and budgets for CO and O<sub>3</sub> in the northeastern Pacific during the spring of 2001: Results from the PHOBEA-II Experiment, *J. Geophys. Res.*, **108**(D20), 8802, doi:10.1029/2002JD003121.
- Jaffe, D., I. McKendry, T. Anderson, and H. Price (2003a), Six 'new' episodes of trans-Pacific transport of air pollutants, *Atmos. Environ.*, **37**, 391–404.
- Jaffe, D., H. Price, D. Parrish, A. Goldstein, and J. Harris (2003b), Increasing background ozone during spring on the west coast of North America, *Geophys. Res. Lett.*, **30**(12), 1613, doi:10.1029/2003GL017024.
- Jaffe, D., J. Snow, and O. Cooper (2003c), The April 2001 Asian dust events: Transport and substantial impact on surface particulate matter concentrations across the United States, *Eos Trans. AGU*, **84**, 501, 507.
- Johnson, B. J., S. J. Oltmans, H. Vömel, H. G. J. Smit, T. Deshler, and C. Kroger (2002), Electrochemical concentration cell (ECC) ozonesonde pump efficiency measurements and tests on the sensitivity to ozone of buffered and unbuffered ECC sensor cathode solutions, *J. Geophys. Res.*, **107**(D19), 4393, doi:10.1029/2001JD000557.
- Komhyr, W. D. (1969), Electrochemical cells for gas analysis, *Ann. Geophys.*, **25**, 203–210.
- Komhyr, W. D., R. A. Barnes, G. B. Brothers, J. A. Lathrop, and D. P. Opperman (1995), Electrochemical concentration cell ozonesonde performance evaluation during STOIC 1989, *J. Geophys. Res.*, **100**, 9231–9244.
- Liang, Q., L. Jaeglé, D. A. Jaffe, P. Weiss-Penzias, A. Heckman, and J. A. Snow (2004), Long-range transport of Asian pollution to the northeast Pacific: Seasonal variations and transport pathways of carbon monoxide, *J. Geophys. Res.*, **109**, D23S07, doi:10.1029/2003JD004402.
- Lin, C.-Y. C., D. J. Jacob, J. W. Munger, and A. M. Fiore (2000), Increasing background ozone in surface over the United States, *Geophys. Res. Lett.*, **27**, 3465–3468.
- Liu, H., D. J. Jacob, I. Bey, R. M. Yantosca, B. N. Duncan, and G. W. Sachse (2003), Transport pathways for Asian pollution outflow over the Pacific: Interannual and seasonal variations, *J. Geophys. Res.*, **108**(D20), 8786, doi:10.1029/2002JD003102.
- Logan, J. A. (1999), An analysis of ozonesonde data for the troposphere: Recommendations for testing 3-D models and development of a gridded climatology for tropospheric ozone, *J. Geophys. Res.*, **104**, 16,115–16,150.
- Marenco, A., et al. (1998), Measurement of ozone and water vapor by Airbus in-service aircraft: The MOZAIC airborne program, An overview, *J. Geophys. Res.*, **103**, 25,631–25,642.
- Newchurch, M. J., M. A. Ayoub, S. Oltmans, B. Johnson, and F. J. Schmidlin (2003), Vertical distribution of ozone at four sites in the United States, *J. Geophys. Res.*, **108**(D1), 4031, doi:10.1029/2002JD002059.
- Nowak, J. B., et al. (2004), Gas-phase chemical characteristics of Asian emission plumes observed during ITCT 2k2 over the eastern North Pacific Ocean, *J. Geophys. Res.*, **109**, D23S19, doi:10.1029/2003JD004488.
- Olivier, J. G. J., and J. J. M. Berdowski (2001), Global emissions of sources and sinks, in *The Climate System*, edited by J. Berdowski, R. Guicherit, and B. J. Heij, pp. 33–78, A. A. Balkema, Brookfield, Vt.
- Oltmans, S. J., et al. (1996), Summer and spring ozone profiles over the North Atlantic from ozonesonde measurements, *J. Geophys. Res.*, **101**, 29,179–29,200.
- Parrish, D. D., Y. Kondo, O. R. Cooper, C. A. Brock, D. A. Jaffe, M. Trainer, G. Hübler, and F. C. Fehsenfeld (2004), Intercontinental Transport and Chemical Transformation 2002 (ITCT-2K2) and Pacific Exploration of Asian Continental Emission (PEACE) experiments: An overview of the 2002 winter and spring intensives, *J. Geophys. Res.*, **109**, D23S01, doi:10.1029/2004JD004980.
- Seibert, P., and A. Frank (2004), Source-receptor matrix calculation with a Lagrangian particle dispersion model in backward mode, *Atmos. Chem. Phys.*, **4**, 51–63.
- Seibert, P., B. Krüger, and A. Frank (2001), Parametrisation of convective mixing in a Lagrangian particle Dispersion model, paper presented at 5th GLOREAM Workshop, Wengen, Switzerland, 24–26 Sept.

- Stohl, A. (1998), Computation, accuracy and applications of trajectories—A review and bibliography, *Atmos. Environ.*, **32**, 947–966.
- Stohl, A. (2001), A 1-year Lagrangian “climatology” of airstreams in the Northern Hemisphere troposphere and lowermost stratosphere, *J. Geophys. Res.*, **106**, 7263–7279.
- Stohl, A., and D. J. Thomson (1999), A density correction for Lagrangian particle dispersion models, *Boundary Layer Meteorol.*, **90**, 155–167.
- Stohl, A., and T. Trickl (1999), A textbook example of long-range transport: Simultaneous observation of ozone maxima of stratospheric and North American origin in the free troposphere over Europe, *J. Geophys. Res.*, **104**, 30,445–30,462.
- Stohl, A., M. Hittenberger, and G. Wotawa (1998), Validation of the Lagrangian particle dispersion model FLEXPART against large scale tracer experiment data, *Atmos. Environ.*, **24**, 4245–4264.
- Stohl, A., S. Eckhardt, C. Forster, P. James, and N. Spichtinger (2002a), On the pathways and timescales of intercontinental air pollution transport, *J. Geophys. Res.*, **107**(D23), 4684, doi:10.1029/2001JD001396.
- Stohl, A., M. Trainer, T. B. Ryerson, J. S. Holloway, and D. D. Parrish (2002b), Export of NO<sub>y</sub> from the North American boundary layer during 1996 and 1997 North Atlantic Regional Experiments, *J. Geophys. Res.*, **107**(D11), 4131, doi:10.1029/2001JD000519.
- Stohl, A., S. Eckhardt, C. Forster, P. James, N. Spichtinger, and P. Seibert (2002c), A replacement for simple back trajectory calculation in the interpretation of atmospheric trace substance measurements, *Atmos. Environ.*, **36**, 4635–4648.
- Stohl, A., C. Forster, S. Eckhardt, N. Spichtinger, H. Huntrieser, J. Heland, H. Schlager, H. Aufmhoff, F. Arnold, and O. Cooper (2003a), A backward modeling study of intercontinental pollution transport using aircraft measurements, *J. Geophys. Res.*, **108**(D12), 4370, doi:10.1029/2002JD002862.
- Stohl, A., et al. (2003b), Rapid intercontinental air pollution transport associated with a meteorological bomb, *Atmos. Chem. Phys.*, **3**, 2101–2141.
- Thouret, V., A. Marenco, J. A. Logan, P. Nédélec, and C. Grouhel (1998), Comparisons of ozone measurements from the MOZAIC airborne program and the ozone sounding network at eight stations, *J. Geophys. Res.*, **103**, 25,695–25,720.
- Yienger, J. J., M. Galanter, T. A. Holloway, M. J. Phadnis, S. K. Guttikunda, G. R. Carmichael, W. J. Moxim, and H. Levy II (2000), The episodic nature of air pollution transport from Asia to North America, *J. Geophys. Res.*, **105**, 26,931–26,945.
- 
- O. R. Cooper, D. D. Parrish, and A. Stohl, Aeronomy Laboratory, NOAA, R/AL4, 325 Broadway, Boulder, CO 80305, USA. (owen.r.cooper@noaa.gov)
- S. Eckhardt, Department of Ecology, Technical University of Munich, D-85354 Freising-Weihenstephan, Germany.
- B. J. Johnson and S. J. Oltmans, Climate Monitoring and Diagnostics Laboratory, NOAA, Boulder, CO 80303, USA.
- K. Kita, Department of Environmental Sciences, Ibaraki University, 310-8512 Ibaraki, Japan.
- Y. Kondo, Research Center for Advanced Science and Technology, University of Tokyo, 153-8904 Tokyo, Japan.
- P. Nédélec, Laboratoire d’Aerologie, CNRS, OMP, 31400 Toulouse, France.
- M. J. Newchurch, Atmospheric Science Department, University of Alabama, Huntsville, AL 35805, USA.
- F. J. Schmidlin, NASA Goddard Space Flight Center, Wallops Flight Facility, Wallops Island, VA 23337, USA.